Fast spectral methods for the shape identification problem of a perfectly conducting obstacle

Frédérique Le Louër *

Abstract

We are concerned with fast methods for the numerical implementation of the direct and inverse scattering problems for a perfectly conducting obstacle. The scattering problem is usually reduced to a single uniquely solvable modified combined-field integral equation (M-CFIE). For the numerical solution of the M-CFIE we propose a new high-order spectral algorithm by transporting this equation on the unit sphere via the Piola transform. The inverse problem is formulated as a nonlinear least squares problem for which the iteratively regularized Gauss-Newton method is applied to recover an approximate solution. Numerical experiments are presented in the special case of star-shaped obstacles.

Keywords : Maxwell equations, perfectly conducting interface, boundary integral equation, spectral method, Fréchet derivative, regularized Newton method.

1 Introduction

In this paper we are concerned with the numerical aspects of the solution of the direct and inverse electromagnetic scattering problems for a three-dimensional bounded and perfectly conducting obstacle lit by time-harmonic incident plane waves.

We assume the perfect conductor be represented by a bounded domain Ω in $\mathbb{R}^3$. Let Ω^c denote the exterior domain $\mathbb{R}^3\backslash\overline{\Omega}$ and $\boldsymbol{n}$ denote the outer unit normal vector to the boundary Γ. Let κ denote the exterior wavenumber. The propagation of electromagnetic waves are governed by the system of Maxwell equations and the time-harmonic Maxwell system can be reduced to a second order equation for the electric field only. In this case the forward problem is formulated as follows : Given an incident electric wave $\boldsymbol{E}^{\mathrm{inc}}$ which is assumed to solve the second order Maxwell equation in the absence of any scatterer, find the electric scattered wave $\boldsymbol{E}^{\mathrm{s}}$ solution to the time-harmonic Maxwell equation

$$\mathbf{curl}\,\mathbf{curl}\,\boldsymbol{E}^{\mathrm{s}} - \kappa^2\boldsymbol{E}^{\mathrm{s}} = 0 \quad \text{in } \Omega^c, \tag{1.1a}$$

and satisfying the boundary condition,

$$\boldsymbol{n}\times(\boldsymbol{E}^{\mathrm{s}} + \boldsymbol{E}^{\mathrm{inc}}) = 0 \qquad \text{on } \Gamma. \tag{1.1b}$$

In addition the scattered field $\boldsymbol{E}^{\mathrm{s}}$ has to satisfy the Silver-Müller radiation condition:

$$\lim_{|\mathbf{x}|\to+\infty} |\mathbf{x}| \left| \mathbf{curl}\,\boldsymbol{E}^{\mathrm{s}}(\mathbf{x}) \times \frac{\mathbf{x}}{|\mathbf{x}|} - i\kappa\boldsymbol{E}^{\mathrm{s}}(\mathbf{x}) \right| = 0. \tag{1.1c}$$

*f.lelouer@math.uni-goettingen.de

This scattering problem can be reduced in several different ways to a single modified combined-field boundary integral equation (M-CFIE). In section 2, we describe, via direct and indirect approaches, the single integral equations that are usually used to solve the problem (1.1a)-(1.1c).

The construction of efficient inverse obstacle scattering algorithm greatly depends on an accurate approximation of the solution to the forward problem. Among all the existing numerical methods to solve integral equations, we focus here on spectral methods. Ganesh and Hawkins already proposed in [8, 9, 10, 11] several spectrally accurate methods to implement the electric field integral equation (EFIE). One of them [11] consists in transporting the EFIE on the unit sphere via a normal transformation acting from the tangent plane to the boundary Γ onto the tangent plane to the unit sphere, so that one only have to seek a solution in terms of tangential vector spherical harmonics. To treat numerically the M-CFIE, we need to implement the hypersingular part of the electromagnetic double layer boundary integral operator. This requires a transformation that move the nullspace of the surface divergence on Γ onto the nullspace of the surface divergence on $\mathbb{S}^2$. The implementation of a hypersingular integral can then be avoided by involving integration by parts and surface derivatives of the vector spherical harmonics that can be computed analytically. Such a transformation is well known as the Piola transform. In section 3 we give the reformulation of the integral equation in spherical coordinates, based on this approach, and describe an appropriate splitting of the various singularities. The fully discrete high order spectral algorithm and numerical examples are presented in section 4. The Piola transform is already used by Hohage and Le Louër [15] to implement systems of second-kind boundary integral equations in an inverse dielectric obstacle scattering algorithm. Therefore, section 3 and 4 use notations and contain various results from [15] that are essential for this paper.

The radiation condition implies that the scattered field $\boldsymbol{E}^s$ has an asymptotic behavior of the form

$$\boldsymbol{E}^s(\mathbf{x}) = \frac{e^{i\kappa|\mathbf{x}|}}{|\mathbf{x}|}\boldsymbol{E}^\infty(\widehat{\mathbf{x}}) + O\left(\frac{1}{|\mathbf{x}|}\right), \quad |\mathbf{x}| \to \infty,$$

uniformly in all directions $\widehat{\mathbf{x}} = \frac{\mathbf{x}}{|\mathbf{x}|}$. The far-field pattern $\boldsymbol{E}^\infty$ is a tangential vector function defined on the unit sphere $\mathbb{S}^2$ of $\mathbb{R}^3$ and is always analytic.

Let consider the scattering of m incident plane waves of the form $\boldsymbol{E}_k^{\mathrm{inc}}(\mathbf{x}) = \boldsymbol{p}_k\, e^{i\kappa\mathbf{x}\cdot\boldsymbol{d}_k}$ where $\boldsymbol{d}_k, \boldsymbol{p}_k \in \mathbb{S}^2$ and $\boldsymbol{d}_k \cdot \boldsymbol{p}_k = 0$. We denote by F_k the boundary to far-field operator that maps the boundary Γ onto the far-field pattern $\boldsymbol{E}_k^\infty$ of the solution to the forward problem (1.1a)-(1.1c) for the incident wave $\boldsymbol{E}_k^{\mathrm{inc}}$. The inverse problem is formulated as follows: Given noisy far field measurements $\boldsymbol{E}_{1,\delta}^\infty, \dots, \boldsymbol{E}_{m,\delta}^\infty$ obtained from the scattering of the m incident plane waves characterized by the couples of directions and polarizations $(\boldsymbol{d}_k, \boldsymbol{p}_k)_{k=1,\dots,m}$, solve

$$F_k(\Gamma) = \boldsymbol{E}_{k,\delta}^\infty, \qquad \text{for } k = 1, \dots, m. \tag{1.2}$$

Here, the noise level is measured in the $\boldsymbol{L}^2$-norm, i.e. $\left(\sum_{k=1}^{m} ||\boldsymbol{E}_{k,\delta}^\infty - \boldsymbol{E}_k^\infty||_{\boldsymbol{L}^2}^2\right)^{\frac{1}{2}} < \delta$, and the error bound δ is assumed to be known. Kress [16] proved that a perfect conductor can be uniquely determined from the knowledge of the far-field pattern for all incoming plane waves. However, it remains an open question whether or not the boundary Γ is uniquely determined by only a finite number of incoming plane waves.

To solve the inverse problem (1.2), we reformulate it as a nonlinear equation posed on an open set of parametrized boundaries. Then we apply the iteratively regularized Gauss-Newton method (IRGNM) to the nonlinear equation via first order linearization. The computation of the iterates requires the analysis and an explicit form of the first Fréchet derivative of the parametrized form of the boundary to far-field operator. The first Fréchet derivative is usually characterized as the far-field pattern of the solution to a new exterior boundary value problem. The fast spectral solver of the direct problem is then incorporated in the IRGNM to compute the far-field pattern of the solution and its derivative at each iteration steps. In electromagnetism, Fréchet differentiability was first investigated by Potthast [21] for the perfect conductor problem, using the boundary integral equation approach. The characterization of the first derivative was then improved by Kress [16]. In section 5, we formulate the IRGNM for the inverse problem (1.2). We also recall the main result on the Fréchet differentiability of the boundary to far-field operator and give a characterization of the adjoint operator, following ideas of [14, 15], which is needed in the implementation of the utilized regularized Newton method. We present numerical experiments in the special case of star-shaped obstacles.

2 The solution of the perfect conductor problem

In this paper, we will assume that the boundary Γ of Ω is a smooth and simply connected closed surface, so that Ω is diffeomorphic to a ball.

Notation: We denote by $H^s(\Omega)$, $H^s_{loc}(\overline{\Omega^c})$ and $H^s(\Gamma)$ the standard (local in the case of the exterior domain) complex valued, Hilbertian Sobolev space of order $s \in \mathbb{R}$ defined on Ω, $\overline{\Omega^c}$ and Γ respectively (with the convention $H^0 = L^2$.) Spaces of vector functions will be denoted by boldface letters, thus $\boldsymbol{H}^s = (H^s)^3$. If P is a differential operator, we write:

$$\begin{aligned}\boldsymbol{H}^s(\mathrm{P},\Omega) &= \{\boldsymbol{v} \in \boldsymbol{H}^s(\Omega) : \mathrm{P}\boldsymbol{v} \in \boldsymbol{H}^s(\Omega)\},\\ \boldsymbol{H}^s_{loc}(\mathrm{P},\overline{\Omega^c}) &= \{\boldsymbol{v} \in \boldsymbol{H}^s_{loc}(\overline{\Omega^c}) : \mathrm{P}\boldsymbol{v} \in \boldsymbol{H}^s_{loc}(\overline{\Omega^c})\}.\end{aligned}$$

The space $\boldsymbol{H}^s(\mathrm{P},\Omega)$ is endowed with the graph norm $||\boldsymbol{v}||_{\boldsymbol{H}^s(\mathrm{P},\Omega)} = \left(||\boldsymbol{v}||^2_{\boldsymbol{H}^s(\Omega)} + ||\mathrm{P}\boldsymbol{v}||^2_{\boldsymbol{H}^s(\Omega)}\right)^{\frac{1}{2}}$. This defines in particular the Hilbert spaces $\boldsymbol{H}^s(\mathbf{curl},\Omega)$ and $\boldsymbol{H}^s(\mathbf{curl}\,\mathbf{curl},\Omega)$ and the Fréchet spaces $\boldsymbol{H}^s_{loc}(\mathbf{curl},\Omega)$ and $\boldsymbol{H}^s_{loc}(\mathbf{curl}\,\mathbf{curl},\Omega)$. When $s = 0$ we omit the upper index 0.

We use the following surface differential operators: The tangential gradient denoted by $\mathbf{grad}_\Gamma$, the surface divergence denoted by div_Γ, the tangential vector curl denoted by $\mathbf{curl}_\Gamma$ and the surface scalar curl denoted by curl_Γ. For their definitions we refer to [15, Appendix A] or [17, pages 68-75]. For $s \in \mathbb{R}$, we introduce the Hilbert space

$$\begin{aligned}\boldsymbol{H}^{\mathrm{s}}_{\mathrm{div}}(\Gamma) &= \{\boldsymbol{j} \in \boldsymbol{H}^{\mathrm{s}}(\Gamma);\ \boldsymbol{j}\cdot\boldsymbol{n} = 0 \text{ and } \mathrm{div}_\Gamma\,\boldsymbol{j} \in H^{\mathrm{s}}(\Gamma)\},\\ \boldsymbol{H}^{\mathrm{s}}_{\mathrm{curl}}(\Gamma) &= \{\boldsymbol{j} \in \boldsymbol{H}^{\mathrm{s}}(\Gamma);\ \boldsymbol{j}\cdot\boldsymbol{n} = 0 \text{ and } \mathrm{curl}_\Gamma\,\boldsymbol{j} \in H^{\mathrm{s}}(\Gamma)\},\end{aligned}$$

endowed with the norms

$$\begin{aligned}||\cdot||_{\boldsymbol{H}^{\mathrm{s}}_{\mathrm{div}}(\Gamma)} &= \left(||\cdot||^2_{\boldsymbol{H}^s(\Gamma)} + ||\,\mathrm{div}_\Gamma\cdot||^2_{H^s(\Gamma)}\right)^{1/2},\\ ||\cdot||_{\boldsymbol{H}^{\mathrm{s}}_{\mathrm{curl}}(\Gamma)} &= \left(||\cdot||^2_{\boldsymbol{H}^s(\Gamma)} + ||\,\mathrm{curl}_\Gamma\cdot||^2_{H^s(\Gamma)}\right)^{1/2}.\end{aligned}$$

Recall that for a vector function $\boldsymbol{u} \in \boldsymbol{H}(\mathbf{curl},\Omega) \cap \boldsymbol{H}(\mathbf{curl}\,\mathbf{curl},\Omega)$, the traces $\boldsymbol{n} \times \boldsymbol{u}_{|\Gamma}$ and $\boldsymbol{n} \times \mathbf{curl}\,\boldsymbol{u}_{|\Gamma}$ are in $\boldsymbol{H}^{-\frac{1}{2}}_{\mathrm{div}}(\Gamma)$. The dual space of $\boldsymbol{H}^{-\frac{1}{2}}_{\mathrm{div}}(\Gamma)$ for the $\boldsymbol{L}^2$ duality product is $\boldsymbol{H}^{-\frac{1}{2}}_{\mathbf{curl}}(\Gamma)$ and the exterior product with the normal vector defines a bicontinuous isomorphism between $\boldsymbol{H}^{-\frac{1}{2}}_{\mathrm{div}}(\Gamma)$ and $\boldsymbol{H}^{-\frac{1}{2}}_{\mathrm{curl}}(\Gamma)$; so that $(\boldsymbol{n} \times \boldsymbol{u}_{|\Gamma}) \times \boldsymbol{n}$ and $(\boldsymbol{n} \times \mathbf{curl}\,\boldsymbol{u}_{|\Gamma}) \times \boldsymbol{n}$ are in $\boldsymbol{H}^{-\frac{1}{2}}_{\mathrm{curl}}(\Gamma)$.

Let $\Phi(\kappa,\mathbf{z}) = \dfrac{e^{i\kappa|\mathbf{z}|}}{4\pi|\mathbf{z}|}$ be the fundamental solution of the Helmholtz equation $\Delta u + \kappa^2 u = 0$. For any solution $\boldsymbol{E}^s$ to the Maxwell equation (1.1a) that satisfies the radiation condition (1.1c), it holds the Stratton-Chu representation formula:

$$\begin{aligned} \boldsymbol{E}^s(\mathbf{x}) = & \int_\Gamma \mathbf{curl}^x \Big\{ \Phi(\kappa, \mathbf{x}-\mathbf{y}) \big(\boldsymbol{n}(\mathbf{y}) \times \boldsymbol{E}^s(\mathbf{y}) \big) \Big\} ds(\mathbf{y}) \\ & + \frac{1}{\kappa^2} \int_\Gamma \mathbf{curl}\,\mathbf{curl}^{\mathbf{x}} \Big\{ \Phi(\kappa, \mathbf{x}-\mathbf{y}) \big(\boldsymbol{n}(\mathbf{y}) \times \mathbf{curl}\, \boldsymbol{E}^s(\mathbf{y}) \big) \Big\} ds(\mathbf{y}). \end{aligned} \tag{2.1}$$

Conversely, for any $\boldsymbol{j} \in \boldsymbol{H}^{-\frac{1}{2}}_{\text{div}}(\Gamma)$ the potentials

$$\mathscr{S}\boldsymbol{j} = \frac{1}{\kappa} \int_\Gamma \mathbf{curl}\,\mathbf{curl}^{\mathbf{x}} \Big\{ \Phi(\kappa, \cdot - \mathbf{y}) \boldsymbol{j}(\mathbf{y}) \big) \Big\} ds(\mathbf{y}) \text{ and } \mathscr{D}\boldsymbol{j} = \int_\Gamma \mathbf{curl}^{\mathbf{x}} \Big\{ \Phi(\kappa, \cdot - \mathbf{y}) \boldsymbol{j}(\mathbf{y}) \Big\} ds(\mathbf{y})$$

satisfy the Maxwell equation and the Silver-Müller radiation condition.

Using these results, the forward problem (1.1a)-(1.1c) can be reduced, in several different ways, to a single uniquely solvable modified combined-field integral equation (M-CFIE). We will consider the following two different approaches. The first one can be used to solve electromagnetic scattering problem with general Dirichlet conditions of the form $\boldsymbol{n} \times \boldsymbol{E}^s = \boldsymbol{f}$ where $\boldsymbol{f} \in \boldsymbol{H}^{-\frac{1}{2}}_{\text{div}}(\Gamma)$ is given. It is based on the layer ansatz :

$$\boldsymbol{E}^s = \mathscr{D}\boldsymbol{j} + i\eta \mathscr{S}\boldsymbol{\Lambda}\boldsymbol{j}, \tag{2.2}$$

where $\boldsymbol{\Lambda}$ is a bounded operator from $\boldsymbol{H}^{-\frac{1}{2}}_{\text{div}}(\Gamma)$ to itself, self-adjoint and elliptic for the bilinear form

$$(\boldsymbol{j}, \boldsymbol{m}) \mapsto \int_\Gamma \boldsymbol{j} \cdot (\boldsymbol{n} \times \boldsymbol{m})\, ds \tag{2.3}$$

and η is a non vanishing real constant. By the jump relations, the field $\boldsymbol{E}^s$ given by (2.2) solves the Dirichlet boundary value problem (1.1a)-(1.1c) if the density $\boldsymbol{j}$ solves the following integral equation

$$(\mathrm{I} - M_\kappa - i\eta C_\kappa \boldsymbol{\Lambda})\boldsymbol{j} = 2\boldsymbol{f} \quad \text{ on } \Gamma. \tag{2.4}$$

Here the single layer potential C_κ and the double layer potential M_κ are defined by

$$\begin{aligned} M_\kappa \boldsymbol{j}(\mathbf{x}) &= -\int_\Gamma \boldsymbol{n}(\mathbf{x}) \times \mathbf{curl}^{\mathbf{x}} \{2\Phi(\kappa, \mathbf{x}-\mathbf{y}) \boldsymbol{j}(\mathbf{y})\} ds(\mathbf{y}), \\ C_\kappa \boldsymbol{j}(\mathbf{x}) &= -\frac{1}{\kappa} \int_\Gamma \boldsymbol{n}(\mathbf{x}) \times \mathbf{curl}\,\mathbf{curl}^{\mathbf{x}} \{2\Phi(\kappa, \mathbf{x}-\mathbf{y}) \boldsymbol{j}(\mathbf{y})\} ds(\mathbf{y}) \\ &= -\kappa\, \boldsymbol{n}(\mathbf{x}) \times \int_\Gamma 2\Phi(\kappa, \mathbf{x}-\mathbf{y}) \boldsymbol{j}(\mathbf{y}) ds(\mathbf{y}) + \frac{1}{\kappa} \mathbf{curl}_\Gamma \int_\Gamma 2\Phi(\kappa, \mathbf{x}-\mathbf{y}) \operatorname{div}_\Gamma \boldsymbol{j}(\mathbf{y}) ds(\mathbf{y}). \end{aligned}$$

The operator $M_\kappa : \boldsymbol{H}^{-\frac{1}{2}}_{\text{div}}(\Gamma) \to \boldsymbol{H}^{-\frac{1}{2}}_{\text{div}}(\Gamma)$ is compact and the operator C_κ has a hypersingular kernel but is bounded on $\boldsymbol{H}^{-\frac{1}{2}}_{\text{div}}(\Gamma)$. The operator $\boldsymbol{\Lambda}$ is then chosen such that $(\mathrm{I} - M_\kappa - C_\kappa \boldsymbol{\Lambda})$ is a Fredholm operator of index zero. Kress first proposed a compact regularization $\boldsymbol{\Lambda}\boldsymbol{j} = \boldsymbol{n} \times S_0^2 \boldsymbol{j}$ where S_0 is the single layer boundary integral operator of the Laplace equation [3], thus $(\mathrm{I} + M_\kappa + C_\kappa \boldsymbol{\Lambda})$ is a Fredhom operator of the second kind. One can also use the elliptic and invertible operator $\boldsymbol{\Lambda}\boldsymbol{j} = C_0 \boldsymbol{j}$ which is a variant of the operator C_κ [5, 22] defined on $\boldsymbol{H}^{-\frac{1}{2}}_{\text{div}}(\Gamma)$ by

$$C_0 \boldsymbol{j} = \boldsymbol{n} \times S_0 \boldsymbol{j} + \mathbf{curl}_\Gamma\, S_0 \operatorname{div}_\Gamma \boldsymbol{j}.$$

The far-field pattern can be computed via the integral representation formula $\boldsymbol{E}^\infty = F_\infty \boldsymbol{j}$ where the far-field operator $F_\infty : \boldsymbol{H}^{-\frac{1}{2}}_{\text{div}}(\Gamma) \to \boldsymbol{L}^2_{\text{t}}(\mathbb{S}^2)$ is defined for $\widehat{\mathbf{x}} \in \mathbb{S}^2$ by :

$$F_\infty \boldsymbol{j}(\widehat{\mathbf{x}}) = \frac{i\kappa}{4\pi} \int_\Gamma e^{-i\kappa \widehat{\mathbf{x}} \cdot \mathbf{y}} \big(\widehat{\mathbf{x}} \times \boldsymbol{j}(\mathbf{y}) \big) ds(\mathbf{y}) + i\eta \frac{\kappa}{4\pi} \int_\Gamma e^{-i\kappa \widehat{\mathbf{x}} \cdot \mathbf{y}} \Big(\big(\widehat{\mathbf{x}} \times \boldsymbol{\Lambda}\boldsymbol{j}(\mathbf{y}) \big) \times \widehat{\mathbf{x}} \Big) ds(\mathbf{y}).$$

The alternative boundary integral equation approach is based on the Stratton-Chu representation formula (2.1) and the following equality for $\mathbf{x} \in \Omega^c$

$$0 = \frac{1}{\kappa^2}\int_\Gamma \mathbf{curl}\,\mathbf{curl}^{\mathbf{x}} \Big\{\Phi(\kappa, \mathbf{x}-\mathbf{y})\big(\boldsymbol{n}(\mathbf{y}) \times \mathbf{curl}\,\boldsymbol{E}^{\text{inc}}(\mathbf{y})\big)\Big\} ds(\mathbf{y})$$
$$+ \int_\Gamma \mathbf{curl}^{x} \Big\{\Phi(\kappa, \mathbf{x}-\mathbf{y})\big(\boldsymbol{n}(\mathbf{y}) \times \boldsymbol{E}^{\text{inc}}(\mathbf{y})\big)\Big\} ds(\mathbf{y}).$$

Adding the last equation to (2.1) and using the boundary condition of $\boldsymbol{E}^s$, it yields

$$\boldsymbol{E}^s(\mathbf{x}) = \frac{1}{\kappa^2}\int_\Gamma \mathbf{curl}\,\mathbf{curl}^{\mathbf{x}} \Big\{\Phi(\kappa, \mathbf{x}-\mathbf{y})\big(\boldsymbol{n}(\mathbf{y}) \times \mathbf{curl}\left(\boldsymbol{E}^s(\mathbf{y}) + \boldsymbol{E}^{\text{inc}}(\mathbf{y})\right)\big)\Big\} ds(\mathbf{y}), \qquad \mathbf{x} \in \Omega^c.$$

Taking the Neumann and Dirichlet trace of the above equation we obtain

$$C_\kappa\left(\frac{1}{\kappa}\boldsymbol{n} \times \mathbf{curl}\left(\boldsymbol{E}^s + \boldsymbol{E}^{\text{inc}}\right)\right) = 2\boldsymbol{n} \times \boldsymbol{E}^{\text{inc}},$$

and

$$(\mathrm{I} + M_\kappa)\left(\frac{1}{\kappa}\boldsymbol{n} \times \mathbf{curl}\left(\boldsymbol{E}^s + \boldsymbol{E}^{\text{inc}}\right)\right) = 2\left(\frac{1}{\kappa}\boldsymbol{n} \times \mathbf{curl}\,\boldsymbol{E}^{\text{inc}}\right).$$

Setting $\boldsymbol{m} = \kappa^{-1}\boldsymbol{n} \times \mathbf{curl}\left(\boldsymbol{E}^s + \boldsymbol{E}^{\text{inc}}\right)$, by a linear combination of the two above equalities we obtain the integral equation

$$(\mathrm{I} + M_\kappa + i\eta\boldsymbol{\Lambda}C_\kappa)\boldsymbol{m} = 2\left(\left(\frac{1}{\kappa}\boldsymbol{n} \times \mathbf{curl}\,\boldsymbol{E}^{\text{inc}}\right) + i\eta\boldsymbol{\Lambda}\big(\boldsymbol{n} \times \boldsymbol{E}^{\text{inc}}\big)\right) \quad \text{on } \Gamma, \tag{2.5}$$

where $\boldsymbol{\Lambda}$ is still an elliptic operator for the bilinear form (2.3).

The far-field pattern can then be computed via the integral representation formula

$$\boldsymbol{E}^\infty(\widehat{\mathbf{x}}) = \frac{\kappa}{4\pi}\int_\Gamma e^{-i\kappa\widehat{\mathbf{x}}\cdot\mathbf{y}}\Big(\big(\widehat{\mathbf{x}} \times \boldsymbol{m}(\mathbf{y})\big) \times \widehat{\mathbf{x}}\Big) ds(\mathbf{y}).$$

3 Spherical reformulation of the integral equation

We transport the surface integral equations (2.4) and (2.5) on a spherical reference domain and work in the spherical coordinate system. We denote by θ, ϕ the spherical coordinates of any point $\widehat{\mathbf{x}} \in \mathbb{S}^2$, that means we can write

$$\widehat{\mathbf{x}} = \psi(\theta, \phi) = (\sin\theta\cos\phi,\ \sin\theta\sin\phi,\ \cos\theta)^\mathsf{T}, \text{ with } (\theta, \phi) \in]0; \pi[\times[0; 2\pi[\cup\{(0,0); (0,\pi)\}.$$

The tangent and the cotangent planes at any point $\widehat{\mathbf{x}} = \psi(\theta, \phi) \in \mathbb{S}^2$ is generated by the unit vectors $\boldsymbol{e}_\theta = \frac{\partial\psi}{\partial\theta}(\theta, \phi)$ and $\boldsymbol{e}_\phi = \frac{1}{\sin\theta}\frac{\partial\psi}{\partial\phi}(\theta, \phi)$. The triplet $(\widehat{\mathbf{x}}, \boldsymbol{e}_\theta, \boldsymbol{e}_\phi)$ forms a direct orthonormal system. The determinant of the Jacobian of the change of variable is $J_\psi(\theta, \phi) = \sin\theta$.

Let $\boldsymbol{q} : \mathbb{S}^2 \to \Gamma$ be a parametrization of class $\mathscr{C}^1$ at least. The total derivative $[\mathbf{D}\boldsymbol{q}(\widehat{\mathbf{x}})]$ maps the tangent plane $\boldsymbol{T}_{\widehat{\mathbf{x}}}$ to $\mathbb{S}^2$ at the point $\widehat{\mathbf{x}}$ onto the tangent plane $\boldsymbol{T}_{\boldsymbol{q}(\widehat{\mathbf{x}})}$ to Γ at the point $\boldsymbol{q}(\widehat{\mathbf{x}})$. The latter is generated by the vectors $\boldsymbol{t}_1(\widehat{\mathbf{x}}) = [\mathbf{D}\boldsymbol{q}(\widehat{\mathbf{x}})]\boldsymbol{e}_\theta$ and $\boldsymbol{t}_2(\widehat{\mathbf{x}}) = [\mathbf{D}\boldsymbol{q}(\widehat{\mathbf{x}})]\boldsymbol{e}_\phi$. The determinant $J_{\boldsymbol{q}}$ of the Jacobian of the change of variable $\boldsymbol{q} : \mathbb{S}^2 \mapsto\in \Gamma$ and the normal vector $\boldsymbol{n} \circ \boldsymbol{q}$ can be computed via the formulas $J_{\boldsymbol{q}} = \left|\boldsymbol{t}_1 \times \boldsymbol{t}_2\right|$ and $\tau_{\boldsymbol{q}}(\boldsymbol{n}) = \frac{\boldsymbol{t}_1 \times \boldsymbol{t}_2}{J_{\boldsymbol{q}}}$. The parametrization $\boldsymbol{q} : \mathbb{S}^2 \to \Gamma$ being a diffeomorphism, we set $[\mathbf{D}\boldsymbol{q}(\widehat{\mathbf{x}})]^{-1} = [\mathbf{D}\boldsymbol{q}^{-1}] \circ \boldsymbol{q}(\widehat{\mathbf{x}})$. The transposed matrix $[\mathbf{D}\boldsymbol{q}(\widehat{\mathbf{x}})^*]^{-1}$ maps the cotangent plane $\boldsymbol{T}^*_{\widehat{\mathbf{x}}}$ to $\mathbb{S}^2$ at the point $\widehat{\mathbf{x}}$ onto the cotangent plane $\boldsymbol{T}^*_{\boldsymbol{q}(\widehat{\mathbf{x}})}$ to Γ at the point $\boldsymbol{q}(\widehat{\mathbf{x}})$. The latter is generated by the vectors $\boldsymbol{t}^1(\widehat{\mathbf{x}}) = \frac{\boldsymbol{t}_2(\boldsymbol{q}(\widehat{\mathbf{x}}))\times \boldsymbol{n}(\boldsymbol{q}(\widehat{\mathbf{x}}))}{J_{\boldsymbol{q}}(\widehat{\mathbf{x}})} = [\mathbf{D}\boldsymbol{q}(\widehat{\mathbf{x}})^*]^{-1}\boldsymbol{e}_\theta$ and $\boldsymbol{t}^2(\widehat{\mathbf{x}}) = \frac{\boldsymbol{n}(\boldsymbol{q}(\widehat{\mathbf{x}}))\times \boldsymbol{t}_1(\boldsymbol{q}(\widehat{\mathbf{x}}))}{J_{\boldsymbol{q}}(\widehat{\mathbf{x}})} = [\mathbf{D}\boldsymbol{q}(\widehat{\mathbf{x}})^*]^{-1}\boldsymbol{e}_\phi$.

To transport the boundary integral equations on the unit sphere, we use the Piola transform of $\boldsymbol{q}$, which is an invertible operator from $\boldsymbol{H}^{-\frac{1}{2}}_{\mathrm{div}}(\Gamma)$ to $\boldsymbol{H}^{-\frac{1}{2}}_{\mathrm{div}}(\mathbb{S}^2)$ defined as follows [15, Lemma 3.1]:

$$\begin{array}{rccc} \mathcal{P}_{\boldsymbol{q}}: & \boldsymbol{H}^{-\frac{1}{2}}_{\mathrm{div}}(\Gamma) & \longrightarrow & \boldsymbol{H}^{-\frac{1}{2}}_{\mathrm{div}}(\mathbb{S}^2) \\ & \boldsymbol{j} & \mapsto & \boldsymbol{j_s} = J_{\boldsymbol{q}}[\mathbf{D}\boldsymbol{q}]^{-1}(\boldsymbol{j}\circ\boldsymbol{q}). \end{array} \tag{3.1}$$

This allows us to use the following identities stated in [15]:

$$\begin{array}{ll} (\mathbf{grad}_\Gamma\, u)\circ\boldsymbol{q} = [\mathbf{D}\boldsymbol{q}^*]^{-1}\,\mathbf{grad}_{\mathbb{S}^2}(u\circ\boldsymbol{q}), & (\mathbf{curl}_\Gamma\, u)\circ\boldsymbol{q} = \dfrac{1}{J_{\boldsymbol{q}}}[\mathbf{D}\boldsymbol{q}]\,\mathbf{curl}_{\mathbb{S}^2}(u\circ\boldsymbol{q}), \\ (\mathrm{div}_\Gamma\, \boldsymbol{v})\circ\boldsymbol{q} = \dfrac{1}{J_{\boldsymbol{q}}}\,\mathrm{div}_{\mathbb{S}^2}\big(J_{\boldsymbol{q}}\,[\mathbf{D}\boldsymbol{q}]^{-1}(\boldsymbol{v}\circ\boldsymbol{q})\big), & (\mathrm{curl}_\Gamma\, \boldsymbol{w})\circ\boldsymbol{q} = \dfrac{1}{J_{\boldsymbol{q}}}\,\mathrm{curl}_{\mathbb{S}^2}\big([\mathbf{D}\boldsymbol{q}^*](\boldsymbol{w}\circ\boldsymbol{q})\big). \end{array} \tag{3.2}$$

The construction of the spectral method is based on the combination of the boundary integral operators M_κ and C_κ with the Piola transform (3.1) and its inverse. In practice, we apply the operator (3.1) to both sides in the boundary integral equations (2.4) and (2.5) and we insert the identity $\mathrm{I}_{\boldsymbol{H}^{-\frac{1}{2}}_{\mathrm{div}}(\Gamma)} = \mathcal{P}_{\boldsymbol{q}}\mathcal{P}_{\boldsymbol{q}}^{-1}$ between the integral operators and the unknown. We thus replace the operators $\boldsymbol{\Lambda}$, M_κ and C_κ in (2.4) and (2.5) by the following operators defined for any density $\boldsymbol{j_s}\in\boldsymbol{H}^{-\frac{1}{2}}_{\mathrm{div}}(\mathbb{S}^2)$ by:

$$\begin{aligned} \boldsymbol{\Lambda_s}\,\boldsymbol{j_s} &= \mathcal{P}_{\boldsymbol{q}}^{-1}\boldsymbol{\Lambda}\mathcal{P}_{\boldsymbol{q}}\boldsymbol{j_s}, \\ \mathcal{M}_\kappa\,\boldsymbol{j_s} &= \mathcal{P}_{\boldsymbol{q}}^{-1}M_\kappa\mathcal{P}_{\boldsymbol{q}}\boldsymbol{j_s} = -J_q[\mathbf{D}\boldsymbol{q}]^{-1}\int_{\mathbb{S}^2}\tau_{\boldsymbol{q}}(\boldsymbol{n})\times\mathbf{curl}\{2\Phi(\kappa,|\boldsymbol{q}(\cdot)-\boldsymbol{q}(\widehat{\mathbf{y}})|)[\mathbf{D}\boldsymbol{q}(\widehat{\mathbf{y}})]\boldsymbol{j_s}(\widehat{\mathbf{y}})\}ds(\widehat{\mathbf{y}}), \\ \mathcal{C}_\kappa\,\boldsymbol{j_s} &= \mathcal{P}_{\boldsymbol{q}}C_\kappa\mathcal{P}_{\boldsymbol{q}}\boldsymbol{j_s} = -\kappa\,J_q[\mathbf{D}\boldsymbol{q}]^{-1}\int_{\mathbb{S}^2}\tau_{\boldsymbol{q}}(\boldsymbol{n})\times\{2\Phi(\kappa,|\boldsymbol{q}(\cdot)-\boldsymbol{q}(\widehat{\mathbf{y}})|)[\mathbf{D}\boldsymbol{q}(\widehat{\mathbf{y}})]\boldsymbol{j_s}(\widehat{\mathbf{y}})\}ds(\widehat{\mathbf{y}}) \\ &\qquad + \frac{1}{\kappa}\,\mathbf{curl}_{\mathbb{S}^2}\int_{\mathbb{S}^2}\{2\Phi(\kappa,|\boldsymbol{q}(\cdot)-\boldsymbol{q}(\widehat{\mathbf{y}})|)\,\mathrm{div}_{\mathbb{S}^2}\,\boldsymbol{j_s}(\widehat{\mathbf{y}})\}ds(\widehat{\mathbf{y}}). \end{aligned}$$

The new unknown will be a tangential vector density in $\boldsymbol{H}^{-\frac{1}{2}}_{\mathrm{div}}(\mathbb{S}^2)$ obtained by applying the Piola transform (3.1) to the unknown in (2.4) or (2.5).

Lemma 3.1 *The operator $\boldsymbol{\Lambda}$ is an elliptic operator on $\boldsymbol{H}^{-\frac{1}{2}}_{\mathrm{div}}(\Gamma)$ for the bilinear form* (2.3) *if and only if $\boldsymbol{\Lambda_s}$ is an elliptic operator on $\boldsymbol{H}^{-\frac{1}{2}}_{\mathrm{div}}(\mathbb{S}^2)$ for the bilinear form*

$$\begin{array}{ccc} \boldsymbol{H}^{-\frac{1}{2}}_{\mathrm{div}}(\mathbb{S}^2)\times\boldsymbol{H}^{-\frac{1}{2}}_{\mathrm{div}}(\mathbb{S}^2) & \rightarrow & \mathbb{C} \\ (\boldsymbol{j_s},\boldsymbol{m}_{\mathrm{s}}) & \mapsto & \displaystyle\int_{\mathbb{S}^2}\boldsymbol{j_s}\cdot(\widehat{\mathbf{x}}\times\boldsymbol{m}_{\mathrm{s}})\,ds \end{array} \tag{3.3}$$

Proof. Let $\boldsymbol{j_s}\in\boldsymbol{H}^{-\frac{1}{2}}_{\mathrm{div}}(\mathbb{S}^2)$. Notice that we have $(\mathcal{P}_{\boldsymbol{q}}^{-1}\boldsymbol{j_s})\circ\boldsymbol{q} = \frac{1}{J_{\boldsymbol{q}}}[\mathbf{D}\boldsymbol{q}]\boldsymbol{j_s}$. In view of the definition of the vectors $\boldsymbol{t}^1$ and $\boldsymbol{t}^2$, we obtain the following equality :

$$\Big(\boldsymbol{n}\times\big(\mathcal{P}_{\boldsymbol{q}}^{-1}\boldsymbol{j_s}\big)\Big)\circ\boldsymbol{q} = [\mathbf{D}\boldsymbol{q}^*]^{-1}\,(\widehat{\mathbf{x}}\times\boldsymbol{j_s})\,. \tag{3.4}$$

Now, we set $\boldsymbol{j} = \mathcal{P}_{\boldsymbol{q}}^{-1}\boldsymbol{j_s}$. We have $\boldsymbol{\Lambda j} = \mathcal{P}_{\boldsymbol{q}}^{-1}\boldsymbol{\Lambda_s j_s}$ and

$$\begin{aligned}\int_\Gamma \boldsymbol{\Lambda j}\cdot(\boldsymbol{n}\times\boldsymbol{j})\,ds &= \int_{\mathbb{S}^2} J_{\boldsymbol{q}}\left((\boldsymbol{\Lambda j})\circ\boldsymbol{q}\right)\cdot\left((\boldsymbol{n}\times\boldsymbol{j})\circ\boldsymbol{q}\right)ds\\ &= \int_{\mathbb{S}^2} J_{\boldsymbol{q}}\Big(\left(\mathcal{P}_{\boldsymbol{q}}^{-1}\boldsymbol{\Lambda_s j_s}\right)\cdot\left(\boldsymbol{n}\times\left(\mathcal{P}_{\boldsymbol{q}}^{-1}\boldsymbol{j_s}\right)\right)\Big)\circ\boldsymbol{q}\,ds\\ &= \int_{\mathbb{S}^2}\left([\mathbf{D}\boldsymbol{q}]\boldsymbol{\Lambda_s j_s}\right)\cdot\Big([\mathbf{D}\boldsymbol{q}^*]^{-1}(\widehat{\mathbf{x}}\times\boldsymbol{j_s})\Big)\,ds\\ &= \int_{\mathbb{S}^2}\boldsymbol{\Lambda_s j_s}\cdot(\widehat{\mathbf{x}}\times\boldsymbol{j_s})\,ds.\end{aligned}$$

It follows that the ellipticity of $\boldsymbol{\Lambda_s}$ for the bilinear form (3.3) results from the ellipticity of $\boldsymbol{\Lambda}$ for the bilinear form (2.3), and conversely. ■

Remark 3.2 *A suitable choice is to define $\boldsymbol{\Lambda_s}$ such that $\boldsymbol{j_s}\mapsto(\boldsymbol{\Lambda_s j_s})\times\widehat{\mathbf{x}}$ is the duality operator from $\boldsymbol{H}_{\mathrm{div}}^{-\frac{1}{2}}(\mathbb{S}^2)$ to $\boldsymbol{H}_{\mathrm{curl}}^{-\frac{1}{2}}(\mathbb{S}^2)$ [17, pp. 208], that is*

$$\boldsymbol{\Lambda_s j}_s = -\nabla_{\mathbb{S}^2}(-\Delta_{\mathbb{S}^2})^{-\frac{3}{2}}\operatorname{curl}_{\mathbb{S}^2} - \mathbf{curl}_{\mathbb{S}^2}(-\Delta_{\mathbb{S}^2})^{-\frac{1}{2}}\operatorname{div}_{\mathbb{S}^2}.$$

In practice we will use the operator defined by $\boldsymbol{\Lambda_s j}_s = \widehat{\mathbf{x}}\times\boldsymbol{j}_s$.

The implementation of the operator $\mathcal{M}_\kappa$ is already discussed in [15]. Here, we focus on the operator $\mathcal{C}_\kappa$. We introduce the functions :

$$\mathcal{S}_1(\boldsymbol{q};\kappa,\widehat{\mathbf{x}},\widehat{\mathbf{y}}) = \frac{1}{2\pi}\cos(\kappa|\boldsymbol{q}(\widehat{\mathbf{x}})-\boldsymbol{q}(\widehat{\mathbf{y}})|),$$

$$\mathcal{S}_2(\boldsymbol{q};\kappa,\widehat{\mathbf{x}},\widehat{\mathbf{y}}) = \frac{1}{2\pi}\begin{cases}\dfrac{\sin(\kappa|\boldsymbol{q}(\widehat{\mathbf{x}})-\boldsymbol{q}(\widehat{\mathbf{y}})|)}{|\boldsymbol{q}(\widehat{\mathbf{x}})-\boldsymbol{q}(\widehat{\mathbf{y}})|} & \widehat{\mathbf{x}}\neq\widehat{\mathbf{y}},\\ \kappa & \widehat{\mathbf{x}}=\widehat{\mathbf{y}}.\end{cases}$$

and

$$R(\boldsymbol{q};\widehat{\mathbf{x}},\widehat{\mathbf{y}}) = \frac{|\widehat{\mathbf{x}}-\widehat{\mathbf{y}}|}{|\boldsymbol{q}(\widehat{\mathbf{x}})-\boldsymbol{q}(\widehat{\mathbf{y}})|}.$$

The operator $\mathcal{C}_\kappa$ can then be rewritten as

$$\begin{aligned}\mathcal{C}_\kappa\,\boldsymbol{j_s}(\widehat{\mathbf{x}}) = &\int_{\mathbb{S}^2}\frac{R(\boldsymbol{q};\widehat{\mathbf{x}},\widehat{\mathbf{y}})}{|\widehat{\mathbf{x}}-\widehat{\mathbf{y}}|}\mathcal{W}_1(\boldsymbol{q};\kappa,\widehat{\mathbf{x}},\widehat{\mathbf{y}})\boldsymbol{j_s}(\widehat{\mathbf{y}})ds(\widehat{\mathbf{y}}) + i\int_{\mathbb{S}^2}\mathcal{W}_2(\boldsymbol{q};\kappa,\widehat{\mathbf{x}},\widehat{\mathbf{y}})\boldsymbol{j_s}(\widehat{\mathbf{y}})ds(\widehat{\mathbf{y}})\\ &+\frac{1}{\kappa}\mathbf{curl}_{\mathbb{S}^2}\int_{\mathbb{S}^2}\frac{R(\boldsymbol{q};\widehat{\mathbf{x}},\widehat{\mathbf{y}})}{|\widehat{\mathbf{x}}-\widehat{\mathbf{y}}|}\mathcal{S}_1(\boldsymbol{q};\kappa,\widehat{\mathbf{x}},\widehat{\mathbf{y}})\operatorname{div}_{\mathbb{S}^2}\boldsymbol{j_s}(\widehat{\mathbf{y}})ds(\widehat{\mathbf{y}})\\ &+\frac{i}{\kappa}\mathbf{curl}_{\mathbb{S}^2}\int_{\mathbb{S}^2}\mathcal{S}_2(\boldsymbol{q};\kappa,\widehat{\mathbf{x}},\widehat{\mathbf{y}})\operatorname{div}_{\mathbb{S}^2}\boldsymbol{j_s}(\widehat{\mathbf{y}})ds(\widehat{\mathbf{y}})\end{aligned}$$

where $\mathcal{W}_1(\boldsymbol{q};\kappa,\widehat{\mathbf{x}},\widehat{\mathbf{y}})$ and $\mathcal{W}_2(\boldsymbol{q};\kappa,\widehat{\mathbf{x}},\widehat{\mathbf{y}})$ are 3×3 matrices given by

$$\begin{aligned}\mathcal{W}_1(\boldsymbol{q};\kappa,\widehat{\mathbf{x}},\widehat{\mathbf{y}}) &= \kappa\mathcal{S}_1(\boldsymbol{q};\kappa,\widehat{\mathbf{x}},\widehat{\mathbf{y}})\mathcal{V}(\boldsymbol{q};\widehat{\mathbf{x}},\widehat{\mathbf{y}}),\\ \mathcal{W}_2(\boldsymbol{q};\kappa,\widehat{\mathbf{x}},\widehat{\mathbf{y}}) &= \kappa\mathcal{S}_2(\boldsymbol{q};\kappa,\widehat{\mathbf{x}},\widehat{\mathbf{y}})\mathcal{V}(\boldsymbol{q};\widehat{\mathbf{x}},\widehat{\mathbf{y}}),\end{aligned}$$

with

$$\begin{aligned}\mathcal{V}(\boldsymbol{q};\widehat{\mathbf{x}},\widehat{\mathbf{y}}) = &\ \boldsymbol{t}_2(\widehat{\mathbf{x}})\cdot\boldsymbol{t}_1(\widehat{\mathbf{y}})\,\boldsymbol{e}_\theta(\widehat{\mathbf{x}})\otimes\boldsymbol{e}_\theta(\widehat{\mathbf{y}}) + \boldsymbol{t}_2(\widehat{\mathbf{x}})\cdot\boldsymbol{t}_2(\widehat{\mathbf{y}})\,\boldsymbol{e}_\theta(\widehat{\mathbf{x}})\otimes\boldsymbol{e}_\phi(\widehat{\mathbf{y}})\\ &-\boldsymbol{t}_1(\widehat{\mathbf{x}})\cdot\boldsymbol{t}_1(\widehat{\mathbf{y}})\,\boldsymbol{e}_\phi(\widehat{\mathbf{x}})\otimes\boldsymbol{e}_\theta(\widehat{\mathbf{y}}) - \boldsymbol{t}_1(\widehat{\mathbf{x}})\cdot\boldsymbol{t}_2(\widehat{\mathbf{y}})\,\boldsymbol{e}_\phi(\widehat{\mathbf{x}})\otimes\boldsymbol{e}_\phi(\widehat{\mathbf{y}}).\end{aligned}$$

Next, we introduce a change of coordinate system in order to move all the singularities in the weakly singular integrals to only one point that is chosen to be the North pole. For $\widehat{\mathbf{x}} \in \mathbb{S}^2$ we consider an orthogonal transformation $T_{\widehat{\mathbf{x}}}$ which maps $\widehat{\mathbf{x}}$ onto the North pole denoted by $\widehat{\boldsymbol{\eta}}$. If $\widehat{\mathbf{x}} = \widehat{\mathbf{x}}(\theta, \phi)$ then $T_{\widehat{\mathbf{x}}} := P(\phi)Q(-\theta)P(-\phi)$ where P and Q are defined by

$$P(\phi) = \begin{pmatrix} \cos\phi & -\sin\phi & 0 \\ \sin\phi & \cos\phi & 0 \\ 0 & 0 & 1 \end{pmatrix} \quad \text{and} \quad Q(\theta) = \begin{pmatrix} \cos\theta & 0 & \sin\phi \\ 0 & 1 & 0 \\ -\sin\phi & 0 & \cos\phi \end{pmatrix}.$$

We also introduce an induced linear tranformation $\mathcal{T}_{\widehat{\mathbf{x}}}$ defined by $\mathcal{T}_{\widehat{\mathbf{x}}} u(\widehat{\mathbf{y}}) = u(T_{\widehat{\mathbf{x}}}^{-1}\widehat{\mathbf{y}})$ and we still denote by $\mathcal{T}_{\widehat{\mathbf{x}}}$ its bivariate analogue $\mathcal{T}_{\widehat{\mathbf{x}}} v(\widehat{\mathbf{y}}_1, \widehat{\mathbf{y}}_2) = v(T_{\widehat{\mathbf{x}}}^{-1}\widehat{\mathbf{y}}_1, T_{\widehat{\mathbf{x}}}^{-1}\widehat{\mathbf{y}}_2)$. If we write $\widehat{\mathbf{z}} = T_{\widehat{\mathbf{x}}}\widehat{\mathbf{y}}$ then we have the identity

$$|\widehat{\mathbf{x}} - \widehat{\mathbf{y}}| = |T_{\widehat{\mathbf{x}}}^{-1}(\widehat{\boldsymbol{\eta}} - \widehat{\mathbf{z}})| = |\widehat{\boldsymbol{\eta}} - \widehat{\mathbf{z}}|.$$

The boundary integral operator $\mathcal{C}_\kappa$ can be rewritten in the form:

$$\begin{aligned} \mathcal{C}_\kappa \, \boldsymbol{j}_{\boldsymbol{s}}(\widehat{\mathbf{x}}) &= \int_{\mathbb{S}^2} \left[\frac{\mathcal{T}_{\widehat{\mathbf{x}}} R(\boldsymbol{q}; \widehat{\boldsymbol{\eta}}, \widehat{\mathbf{z}})}{|\widehat{\boldsymbol{\eta}} - \widehat{\mathbf{z}}|} \mathcal{T}_{\widehat{\mathbf{x}}} \mathcal{W}_1(\boldsymbol{q}; \kappa, \widehat{\boldsymbol{\eta}}, \widehat{\mathbf{z}}) + i \mathcal{T}_{\widehat{\mathbf{x}}} \mathcal{W}_2(\boldsymbol{q}; \kappa, \widehat{\boldsymbol{\eta}}, \widehat{\mathbf{z}}) \right] \mathcal{T}_{\widehat{\mathbf{x}}} \boldsymbol{j}_{\boldsymbol{s}}(\widehat{\mathbf{z}}) ds(\widehat{\mathbf{z}}) \\ + \frac{1}{\kappa} \, \mathbf{curl}_{\mathbb{S}^2} & \int_{\mathbb{S}^2} \left(\frac{\mathcal{T}_{\widehat{\mathbf{x}}} R(\boldsymbol{q}; \widehat{\boldsymbol{\eta}}, \widehat{\mathbf{z}})}{|\widehat{\boldsymbol{\eta}} - \widehat{\mathbf{z}}|} \mathcal{T}_{\widehat{\mathbf{x}}} \mathcal{S}_1(\boldsymbol{q}; \kappa, \widehat{\boldsymbol{\eta}}, \widehat{\mathbf{z}}) + i \mathcal{T}_{\widehat{\mathbf{x}}} \mathcal{S}_2(\boldsymbol{q}; \kappa, \widehat{\boldsymbol{\eta}}, \widehat{\mathbf{z}}) \right) \mathcal{T}_{\widehat{\mathbf{x}}} \big(\operatorname{div}_{\mathbb{S}^2} \boldsymbol{j}_{\boldsymbol{s}} \big)(\widehat{\mathbf{z}}) ds(\widehat{\mathbf{z}}), \end{aligned} \tag{3.5}$$

and it can be shown that the mappings $(\theta', \phi') \mapsto \mathcal{T}_{\widehat{\mathbf{x}}} R(\boldsymbol{q}; \widehat{\boldsymbol{\eta}}, \widehat{\mathbf{z}}(\theta', \phi')) \mathcal{T}_{\widehat{\mathbf{x}}} \mathcal{S}_1(\boldsymbol{q}; \kappa, \widehat{\boldsymbol{\eta}}, \widehat{\mathbf{z}}(\theta', \phi'))$ and $(\theta', \phi') \mapsto \mathcal{T}_{\widehat{\mathbf{x}}} R(\boldsymbol{q}; \widehat{\boldsymbol{\eta}}, \widehat{\mathbf{z}}(\theta', \phi')) \mathcal{T}_{\widehat{\mathbf{x}}} \mathcal{C}_1(\boldsymbol{q}; \kappa, \widehat{\boldsymbol{\eta}}, \widehat{\mathbf{z}}(\theta', \phi'))$ are smooth. An important point is that the singularity $\frac{1}{|\widehat{\boldsymbol{\eta}} - \widehat{\mathbf{z}}(\theta', \phi')|} = \frac{1}{2 \sin \frac{\theta'}{2}}$ is cancelled out by the surface element $ds(\widehat{\mathbf{z}}) = \sin\theta' d\theta' d\phi'$.

Finally, setting $\boldsymbol{f}_{\boldsymbol{s}} = \mathcal{P}_{\boldsymbol{q}} \boldsymbol{f}$, the parametrized form of the equation (2.4) is

$$\Big(\mathrm{I}_{\boldsymbol{H}_{\mathrm{div}}^{-\frac{1}{2}}(\mathbb{S}^2)} - \mathcal{M}_\kappa - i\eta \mathcal{C}_\kappa \boldsymbol{\Lambda}_{\boldsymbol{s}} \Big) \boldsymbol{j}_{\boldsymbol{s}} = 2 \boldsymbol{f}_{\boldsymbol{s}}, \quad \text{on } \mathbb{S}^2, \tag{3.6}$$

and setting $\boldsymbol{u}_1^{\mathrm{inc}} = \mathcal{P}_{\boldsymbol{q}} \big(\boldsymbol{n} \times \boldsymbol{E}^{\mathrm{inc}} \big)$ and $\boldsymbol{u}_2^{\mathrm{inc}} = \mathcal{P}_{\boldsymbol{q}} \big(\boldsymbol{n} \times \mathbf{curl}\, \boldsymbol{E}^{\mathrm{inc}} \big)$ the parametrized form of the equation (2.5) is

$$\Big(\mathrm{I}_{\boldsymbol{H}_{\mathrm{div}}^{-\frac{1}{2}}(\mathbb{S}^2)} + \mathcal{M}_\kappa + i\eta \boldsymbol{\Lambda}_{\boldsymbol{s}} \mathcal{C}_\kappa \Big) \boldsymbol{j}_{\boldsymbol{s}} = 2 \left(\Big(\frac{1}{\kappa} \boldsymbol{u}_2^{\mathrm{inc}} \Big) + i\eta \boldsymbol{\Lambda}_{\boldsymbol{s}} \boldsymbol{u}_1^{\mathrm{inc}} \right), \quad \text{on } \mathbb{S}^2. \tag{3.7}$$

4 A high order spectral algorithm

The parametrized boundary integral equations (3.6) and (3.7) are now propicious to obtain spectrally accurate approximations of the solution by combining the spectral method of Ganesh and Graham [7] and the hybrid spectral method of Ganesh and Hawkins [10, 11]. The numerical scheme is based on the numerical integration formula over the unit sphere for a continuous function

$$\int_{\mathbb{S}^2} u(\widehat{\mathbf{x}}) ds(\widehat{\mathbf{x}}) \approx \sum_{\rho=0}^{2n+1} \sum_{\tau=1}^{n+1} \mu_\rho \nu_\tau u(\widehat{\mathbf{x}}(\theta_\tau, \phi_\rho)), \tag{4.1}$$

where $\theta_\tau = \arccos \zeta_\tau$ where ζ_τ, for $\tau = 1, \ldots, n+1$, are the zeros of the Legendre polynomial P_{n+1}^0 of degree $n+1$ and ν_τ, for $\tau = 1, \ldots, n+1$, are the corresponding Gauss-Legendre weights and

$$\mu_\rho = \frac{\pi}{n+1}, \quad \phi_\rho = \frac{\rho\pi}{n+1}, \quad \text{for } \rho = 0, \ldots, 2n+1.$$

For $l \in \mathbb{N}$ and $0 \le j \le l$, let P_l^j denote the j-th associated Legendre function of order l. When $j = 0$ we write $P_l^0 = P_l$. The spherical harmonics defined by

$$Y_{l,j}(\widehat{\mathbf{x}}) = (-1)^{\frac{|j|+j}{2}} \sqrt{\frac{2l+1}{4\pi} \frac{(l-|j|!)}{(l+|j|!)}} P_l^{|j|}(\cos\theta) e^{ij\phi}$$

for $j = -l, \ldots, l$ and $l = 0, 1, 2, \ldots$ form a complete orthonormal system in $L^2(\mathbb{S}^2)$. The formula (4.1) is exact for the spherical polynomials of order less than or equal to $2n+1$ (see [20]). This induces the discrete inner product $(\cdot,\cdot)_n$

$$(\varphi_1, \varphi_2)_n = \sum_{\rho=0}^{2n+1} \sum_{\tau=1}^{n+1} \mu_\rho \nu_\tau \varphi_1(\widehat{\mathbf{x}}_{\rho\tau}) \overline{\varphi_2(\widehat{\mathbf{x}}_{\rho\tau})},$$

on the space $\mathbb{P}_n$ of all scalar spherical polynomials of degree less than or equal to n. We have $(\varphi_1, \varphi_2)_{\mathbb{S}^2} = (\varphi_1, \varphi_2)_n$ for all $\varphi_1, \varphi_2 \in \mathbb{P}_n$. We introduce a projection operator ℓ_n on $\mathbb{P}_n$ defined by

$$\ell_n u = \sum_{l=0}^{n} \sum_{j=-l}^{l} (u, Y_{l,j})_n Y_{l,j},$$

and we set

$$\mathscr{L}_n \boldsymbol{u} = \begin{pmatrix} \ell_n u_1 \\ \ell_n u_2 \\ \ell_n u_3 \end{pmatrix} \text{ where } \boldsymbol{u} = (u_1, u_2, u_3)^{\mathsf{T}}.$$

The tangential vector spherical harmonics defined by

$$\boldsymbol{\mathcal{Y}}_{l,j}^{(1)} = \frac{1}{\sqrt{l(l+1)}} \,\mathbf{grad}_{\mathbb{S}^2} Y_{l,j} \text{ and } \boldsymbol{\mathcal{Y}}_{l,j}^{(2)} = \frac{1}{\sqrt{l(l+1)}} \,\mathbf{curl}_{\mathbb{S}^2} Y_{l,j}$$

for $j = -l, \ldots, l$ and $l = 1, 2, \ldots$ form a complete orthonormal system in $\boldsymbol{L}_{\mathrm{t}}^2(\mathbb{S}^2)$. The formula (4.1) is exact for the vector spherical polynomials of order less than or equal to $2n$ and we have $\boldsymbol{\mathcal{Y}}_{l,j}^{(k)} \cdot \boldsymbol{\mathcal{Y}}_{l',j'}^{(k')} \in \mathbb{P}_{2n+1}$ for $l, l' \le n$, $|j| \le l$, $|j'| \le l'$ and $k, k' = 1, 2$ (see [20]). This induces the discrete inner product

$$(\boldsymbol{v}_1 | \boldsymbol{v}_2)_n = \sum_{\rho=0}^{2n+1} \sum_{\tau=1}^{n+1} \mu_\rho \nu_\tau \boldsymbol{v}_1(\widehat{\mathbf{x}}_{\rho\tau}) \cdot \overline{\boldsymbol{v}_2(\widehat{\mathbf{x}}_{\rho\tau})},$$

on the subspace $\mathbb{T}_n \subset \boldsymbol{H}_{\mathrm{div}}^{-\frac{1}{2}}(\mathbb{S}^2)$ of finite dimension $2(n+1)^2 - 2$ generated by the orthonormal basis of tangential vector spherical harmonics of degree less than or equal to $n \in \mathbb{N}$. We introduce a projection operator $\boldsymbol{\mathcal{L}}_n$ on $\mathbb{T}_n$ defined by

$$\boldsymbol{\mathcal{L}}_n \boldsymbol{v} = \sum_{i=1}^{2} \sum_{l=1}^{n} \sum_{j=-l}^{l} (\boldsymbol{v} | \boldsymbol{\mathcal{Y}}_{lj}^{(i)})_n \boldsymbol{\mathcal{Y}}_{lj}^{(i)}.$$

In a first step, the operator $\mathcal{C}_\kappa$ is approached by

$$\begin{aligned}
\mathcal{C}_{\kappa,n'} \,\boldsymbol{j_s}(\widehat{\mathbf{x}}) = & \int_{\mathbb{S}^2} \frac{1}{|\hat{\boldsymbol{\eta}} - \widehat{\mathbf{z}}|} \mathscr{L}_{n'} \{\mathcal{T}_{\widehat{\mathbf{x}}} R(\boldsymbol{q}; \hat{\boldsymbol{\eta}}, \cdot) \mathcal{T}_{\widehat{\mathbf{x}}} \mathcal{W}_1(\boldsymbol{q}; \kappa, \hat{\boldsymbol{\eta}}, \cdot) \mathcal{T}_{\widehat{\mathbf{x}}} \boldsymbol{j_s}(\cdot)\}(\widehat{\mathbf{z}}) ds(\widehat{\mathbf{z}}) \\
& + i \int_{\mathbb{S}^2} \mathscr{L}_{n'} \{\mathcal{T}_{\widehat{\mathbf{x}}} \mathcal{W}_2(\boldsymbol{q}; \kappa, \hat{\boldsymbol{\eta}}, \cdot) \mathcal{T}_{\widehat{\mathbf{x}}} \boldsymbol{j_s}(\cdot)\}(\widehat{\mathbf{z}}) ds(\widehat{\mathbf{z}}) \\
& + \frac{1}{\kappa} \,\mathbf{curl}_{\mathbb{S}^2} \int_{\mathbb{S}^2} \frac{1}{|\hat{\boldsymbol{\eta}} - \widehat{\mathbf{z}}|} \ell_{n'} \{\mathcal{T}_{\widehat{\mathbf{x}}} R(\boldsymbol{q}; \widehat{\mathbf{x}}, \cdot) \mathcal{T}_{\widehat{\mathbf{x}}} \mathcal{S}_1(\boldsymbol{q}; \kappa, \widehat{\mathbf{x}}, \cdot) \mathcal{T}_{\widehat{\mathbf{x}}} \big(\operatorname{div}_{\mathbb{S}^2} \boldsymbol{j_s}(\cdot)\big)\}(\widehat{\mathbf{z}}) ds(\widehat{\mathbf{z}}) \\
& + \frac{i}{\kappa} \,\mathbf{curl}_{\mathbb{S}^2} \int_{\mathbb{S}^2} \ell_{n'} \{\mathcal{T}_{\widehat{\mathbf{x}}} \mathcal{S}_2(\boldsymbol{q}; \kappa, \widehat{\mathbf{x}}, \cdot) \mathcal{T}_{\widehat{\mathbf{x}}} \big(\operatorname{div}_{\mathbb{S}^2} \boldsymbol{j_s}(\cdot)\big)\}(\widehat{\mathbf{z}}) ds(\widehat{\mathbf{z}}).
\end{aligned}$$

for some $n' = an + 1$ with fixed $a > 1$ and $n' - n > 3$ (see [11] and [8, Appendix A]). By the use of the fact that the scalar spherical harmonics are eigenfunctions of the single layer potential on the sphere and additional identities [4] we obtain

$$\mathcal{C}_{\kappa,n'}\, \boldsymbol{j_s}(\widehat{\mathbf{x}}) = \mathcal{W}_{\kappa,n'}\, \boldsymbol{j_s}(\widehat{\mathbf{x}}) + \frac{1}{\kappa}\,\mathbf{curl}_{\mathbb{S}^2}\, \mathcal{S}_{\kappa,n'}\, \mathrm{div}_{\mathbb{S}^2}\, \boldsymbol{j_s}(\widehat{\mathbf{x}}), \tag{4.2}$$

with

$$\begin{aligned}\mathcal{W}_{\kappa,n'}\, \boldsymbol{j_s}(\widehat{\mathbf{x}}) = &\sum_{\rho'=0}^{2n'+1}\sum_{\tau'=1}^{n'+1} \mu_{\rho'}\nu_{\tau'}\alpha_{\tau'}\mathcal{T}_{\widehat{\mathbf{x}}}R(\boldsymbol{q};\hat{\boldsymbol{\eta}},\widehat{\mathbf{z}}_{\rho'\tau'})\mathcal{T}_{\widehat{\mathbf{x}}}\mathcal{W}_1(\boldsymbol{q};\kappa,\hat{\boldsymbol{\eta}},\widehat{\mathbf{z}}_{\rho'\tau'})\mathcal{T}_{\widehat{\mathbf{x}}}\boldsymbol{j_s}(\widehat{\mathbf{z}}_{\rho'\tau'})\\ &+ i\sum_{\rho'=0}^{2n'+1}\sum_{\tau'=1}^{n'+1} \mu_{\rho'}\nu_{\tau'}\mathcal{T}_{\widehat{\mathbf{x}}}\mathcal{W}_2(\boldsymbol{q};\kappa,\hat{\boldsymbol{\eta}},\widehat{\mathbf{z}}_{\rho'\tau'})\mathcal{T}_{\widehat{\mathbf{x}}}\boldsymbol{j_s}(\widehat{\mathbf{z}}_{\rho'\tau'}),\end{aligned}$$

and

$$\begin{aligned}\mathcal{S}_{\kappa,n'}\, \varphi_{\boldsymbol{s}}(\widehat{\mathbf{x}}) = &\sum_{\rho'=0}^{2n'+1}\sum_{\tau'=1}^{n'+1} \mu_{\rho'}\nu_{\tau'}\alpha_{\tau'}\mathcal{T}_{\widehat{\mathbf{x}}}R(\boldsymbol{q};\hat{\boldsymbol{\eta}},\widehat{\mathbf{z}}_{\rho'\tau'})\mathcal{T}_{\widehat{\mathbf{x}}}\mathcal{S}_1(\boldsymbol{q};\kappa,\hat{\boldsymbol{\eta}},\widehat{\mathbf{z}}_{\rho'\tau'})\mathcal{T}_{\widehat{\mathbf{x}}}\varphi_{\boldsymbol{s}}(\widehat{\mathbf{z}}_{\rho'\tau'})\\ &+ i\sum_{\rho'=0}^{2n'+1}\sum_{\tau'=1}^{n'+1} \mu_{\rho'}\nu_{\tau'}\mathcal{T}_{\widehat{\mathbf{x}}}\mathcal{S}_2(\boldsymbol{q};\kappa,\hat{\boldsymbol{\eta}},\widehat{\mathbf{z}}_{\rho'\tau'})\mathcal{T}_{\widehat{\mathbf{x}}}\varphi_{\boldsymbol{s}}(\widehat{\mathbf{z}}_{\rho'\tau'}),\end{aligned}$$

where $\alpha_{\tau'} = \sum_{l=0}^{n'} P_l(\zeta_{\tau'})$. We proceed in the same way for the operator $\mathcal{M}_\kappa$ as for the weakly singular part of $\mathcal{C}_\kappa$ and we denote by $\mathcal{M}_{\kappa,n'}$ its approximation. Our fully discrete scheme for (3.6) is as follows: compute $\boldsymbol{j}_n \in \mathbb{T}_n$ such that

$$\boldsymbol{j}_n - \boldsymbol{\mathcal{L}}_n\mathcal{M}_{\kappa,n'}\boldsymbol{j}_n - i\eta\boldsymbol{\mathcal{L}}_n\mathcal{C}_{\kappa,n'}\boldsymbol{\Lambda_s}\boldsymbol{j}_n = 2\boldsymbol{\mathcal{L}}_n\boldsymbol{f_s}, \tag{4.3}$$

where $\boldsymbol{\Lambda_s}$ is defined as in remark 3.2. Since any density $\boldsymbol{j}_n \in \mathbb{T}_n$ can be written

$$\boldsymbol{j}_n = \sum_{l=1}^{n}\sum_{j=-l}^{l} \alpha_{l,j}\boldsymbol{\mathcal{Y}}_{l,j}^{(1)} + \beta_{l,j}\boldsymbol{\mathcal{Y}}_{l,j}^{(2)},$$

the equation (4.3) is equivalent to a system of $2\times\big((n+1)^2-1\big)$ equations for the $2\times\big((n+1)^2-1\big)$ unknown coefficients $(\alpha_{l,j})$ and $(\beta_{l,j})$ by applying the scalar product $(\,\cdot\,|\boldsymbol{\mathcal{Y}}_{l,j}^{(1)})_n$ and $(\,\cdot\,|\boldsymbol{\mathcal{Y}}_{l,j}^{(2)})_n$, for $l = 1,\dots,n$ and $j = -l,\dots,l$ to the equation (4.3). The same remarks hold true for the equation (3.7).

In the remaining of the section we briefly describe the fully discrete scheme for the equation (4.3) and give numerical results. The discrete approximation $\mathbf{W}_\kappa$ of the weakly singular part of the operator of $\mathcal{C}_\kappa$ is of the form

$$\mathbf{W}_\kappa = \begin{pmatrix}\mathbf{W}_{1,1} & \mathbf{W}_{1,2}\\ \mathbf{W}_{2,1} & \mathbf{W}_{2,2}\end{pmatrix},$$

where $\mathbf{W}_{a,b}$, for $a,b = 1,2$ is a $\big((n+1)^2-1\big)\times\big((n+1)^2-1\big)$ matrix. The coefficients of $\mathbf{W}_{a,b}$, for $1 \le l,l' \le n$, $|j| \le l$ and $|j'| \le l'$ are given by

$$\mathbf{W}_{a,b}^{ljl'j'} = (\boldsymbol{\mathcal{L}}_n\mathcal{W}_{\kappa,n'}\boldsymbol{\mathcal{Y}}_{l,j}^{(b)}|\boldsymbol{\mathcal{Y}}_{l'j'}^{(a)})_n.$$

The discrete approximation of the operator $\mathcal{M}_\kappa$ is obtained in the same way and is denoted by $\mathbf{M}_\kappa$. We refer to the paper of Hohage and Le Louër [15] for details on their numerical implementation. The discrete approximation of the hypersingular part of the operator $\mathcal{C}_\kappa$ is of the form

$$\mathbf{H}_\kappa = \begin{pmatrix} 0 & 0 \\ \mathbf{H}_{2,1} & 0 \end{pmatrix},$$

where $\mathbf{T}_{2,1}$ is a $\big((n+1)^2-1\big)\times\big((n+1)^2-1\big)$ matrix. The coefficients of $\mathbf{H}_{2,1}$, for $1\leq l,l'\leq n$, $|j|\leq l$ and $|j'|\leq l'$ are given by

$$\begin{aligned}\mathbf{H}_{2,1}^{ljl'j'} &= \kappa^{-1}(\boldsymbol{\mathcal{L}}_n\,\mathbf{curl}_{\mathbb{S}^2}\,\mathcal{S}_{\kappa,n'}\,\mathrm{div}_{\mathbb{S}^2}\,\boldsymbol{\mathcal{Y}}_{l,j}^{(1)}|\boldsymbol{\mathcal{Y}}_{l'j'}^{(2)})_n\\ &= -\kappa^{-1}(\mathbf{curl}_{\mathbb{S}^2}\,\ell_n\mathcal{S}_{\kappa,n'}\sqrt{l(l+1)}Y_{l,j},\boldsymbol{\mathcal{Y}}_{l'j'}^{(2)})_n\\ &= -\kappa^{-1}(\ell_n\mathcal{S}_{\kappa,n'}\sqrt{l(l+1)}Y_{l,j},\sqrt{l'(l'+1)}Y_{l'j'})_n\,.\end{aligned}$$

where $\mathcal{S}_{\kappa,n'}$ is the discrete approximation of the acoustic single layer potential and we refer to the paper of Ganesh and Graham [7] for details on its numerical implementation. The discrete approximation of the operator $\mathcal{C}_\kappa$ is $\mathbf{C}_\kappa=\mathbf{W}_\kappa+\mathbf{H}_\kappa$. The discrete approximation of $\boldsymbol{\Lambda}_s$ is of the form

$$\boldsymbol{\Lambda}_n = \begin{pmatrix} 0 & -\mathrm{I}_{\mathbb{C}^{(n+1)^2-1}} \\ \mathrm{I}_{\mathbb{C}^{(n+1)^2-1}} & 0 \end{pmatrix}.$$

Finaly, the discrete approximation of the integral operator associated to (2.4) is $\mathrm{I}-\mathbf{M}_\kappa-i\eta\mathbf{C}_\kappa\boldsymbol{\Lambda}_n$, and the discrete approximation of the integral operator associated to (2.5) is $\mathrm{I}+\mathbf{M}_\kappa+i\eta\boldsymbol{\Lambda}_n\mathbf{C}_\kappa$. The discrete approximation of the right-hand side $2\boldsymbol{f_s}=2\mathcal{P}_{\boldsymbol{q}}\boldsymbol{f}$ of one of the boundary integral equations is the vector $2\mathbf{f}$, where $\mathbf{f}=(\mathbf{f}_1,\mathbf{f}_2)^\top$, whose coefficients are given for $k=1,2$, $l=1,\dots,n$ and $j=-l,\dots,l$ by $\mathbf{f}_k^{lj}=(\boldsymbol{\mathcal{L}}_n\mathcal{P}_{\boldsymbol{q}}\boldsymbol{f}|\boldsymbol{\mathcal{Y}}_{lj}^{(k)})_n$.

The parametrized form of the far-field operator F_∞ is $\mathcal{F}_\infty\boldsymbol{j_s}=\mathcal{F}_1\,\boldsymbol{j_s}+i\eta\mathcal{F}_2\,\boldsymbol{\Lambda}_s\boldsymbol{j_s}$, with

$$(\mathcal{F}_1\boldsymbol{j_s})(\widehat{\mathbf{x}}) = \frac{i\kappa}{4\pi}\int_{\mathbb{S}^2} e^{-i\kappa\widehat{\mathbf{x}}\cdot\boldsymbol{q}(\widehat{\mathbf{y}})}\Big(\big(\boldsymbol{e}_\theta(\widehat{\mathbf{y}})\cdot\boldsymbol{j_s}(\widehat{\mathbf{y}})\big)\widehat{\mathbf{x}}\times\boldsymbol{t}_1(\widehat{\mathbf{y}})+\big(\boldsymbol{e}_\phi(\widehat{\mathbf{y}})\cdot\boldsymbol{j_s}(\widehat{\mathbf{y}})\big)\widehat{\mathbf{x}}\times\boldsymbol{t}_2(\widehat{\mathbf{y}})\Big)ds(\widehat{\mathbf{y}}),$$

and

$$(\mathcal{F}_2\boldsymbol{m}_\mathrm{s})(\widehat{\mathbf{x}}) = \frac{\kappa}{4\pi}\int_{\mathbb{S}^2} e^{-i\kappa\widehat{\mathbf{x}}\cdot\boldsymbol{q}(\widehat{\mathbf{y}})}\Big(\big(\boldsymbol{e}_\theta(\widehat{\mathbf{y}})\cdot\boldsymbol{m}_\mathrm{s}(\widehat{\mathbf{y}})\big)\widehat{\mathbf{x}}\times\boldsymbol{t}_1(\widehat{\mathbf{y}})+\big(\boldsymbol{e}_\phi(\widehat{\mathbf{y}})\cdot\boldsymbol{m}_\mathrm{s}(\widehat{\mathbf{y}})\big)\widehat{\mathbf{x}}\times\boldsymbol{t}_2(\widehat{\mathbf{y}})\Big)\times\widehat{\mathbf{x}}\,ds(\widehat{\mathbf{y}}).$$

The discrete approximation of $\mathcal{F}_\infty$ evaluated at the $2(n_\infty+1)^2$ Gauss-quadrature points on the unit far sphere is

$$\mathbf{F}_\infty = \begin{pmatrix}\mathbf{F}_1 & \mathbf{F}_2\end{pmatrix}\begin{pmatrix}\mathrm{I}_{\mathbb{C}^{2(n+1)^2-2}} & 0\\ 0 & \boldsymbol{\Lambda}_n\end{pmatrix}$$

with

$$\mathbf{F}_1 = \begin{pmatrix}\mathbf{F}_{1,1} & \mathbf{F}_{1,2}\end{pmatrix},\quad \mathbf{F}_2 = \begin{pmatrix}\mathbf{F}_{2,1} & \mathbf{F}_{2,2}\end{pmatrix}$$

where $\mathbf{F}_{a,b}$, for $a,b=1,2$ is a $6(n_\infty+1)^2\times((n+1)^2-1)$ matrix. The coefficients of $\mathbf{F}_{a,b}$, for $a,b=1,2$, $1\leq l'\leq n$, $|j'|\leq l'$ and $\rho=0,\dots,2n_\infty+1$ and $\tau=1,\dots,n_\infty+1$ are given by $\mathbf{F}_{a,b}^{\rho\tau l'j'}=\Big(\mathcal{F}_a\boldsymbol{\mathcal{Y}}_{l'j'}^{(b)}\Big)(\widehat{\mathbf{x}}_{\rho\tau})$.

Table 2 exhibits emphasized fast convergence for the far-field pattern $\boldsymbol{E}^\infty$ for boundaries with parametric representations given in Table 1. As a first test we compute the electric far-field denoted, $\boldsymbol{E}_{\mathrm{ps}}^\infty$, created by an off center point source located inside the perfect conductor :

$$\boldsymbol{E}^{\mathrm{inc}}(\mathbf{x}) = \mathbf{grad}\,\Phi(\kappa,|\mathbf{x}-\boldsymbol{s}|)\times\boldsymbol{p},\quad \boldsymbol{s}\in\Omega \text{ and } \boldsymbol{p}\in\mathbb{S}^2.$$

Table 1: Parametric representation of the perfectly conducting obstacles [1, 18]

surface	parametric representation
sphere	$\boldsymbol{q}\circ\psi(\theta,\phi)=R\psi(\theta,\phi),\ R\in\mathbb{R}_+^*;$
great stellated dodecahedron	$\boldsymbol{q}\circ\psi(\theta,\phi)=0.33\,r(\theta,\phi)\psi(\theta,\phi)$, where $r(\theta,\phi)>0$ solves $p^{-\lvert r(\theta,\phi)f(\delta,\xi,0)\rvert^p}+p^{-\lvert r(\theta,\phi)f(\delta,-\xi,0)\rvert^p}+p^{-\lvert r(\theta,\phi)f(0,\delta,\xi)\rvert^p}$ $+p^{-\lvert r(\theta,\phi)f(0,\delta,-\xi)\rvert^p}+p^{-\lvert r(\theta,\phi)f(\xi,0,\delta)\rvert^p}+p^{-\lvert r(\theta,\phi)f(-\xi,0,\delta)\rvert^p}=2.5,$ with $f(a,b,c)=a\sin\theta\cos\phi+b\sin\theta\sin\phi+c\cos\theta,$ $\delta=\sqrt{\frac{5-\sqrt{5}}{10}},\ \xi=\sqrt{\frac{5+\sqrt{5}}{10}},\ p\in\mathbb{N},\ p>2.$

Table 2: Numerical examples for the perfect conductor problem

surface	n	$\lvert\lvert[\boldsymbol{E}^\infty_{\text{ps}}]_n-\boldsymbol{E}^\infty_{\text{exact}}\rvert\rvert_\infty$	$\text{Re}[\boldsymbol{E}^\infty_{\text{pw}}(\boldsymbol{d})]_n\cdot\boldsymbol{p}$	$\text{Im}[\boldsymbol{E}^\infty_{\text{pw}}(\boldsymbol{d})]_n\cdot\boldsymbol{p}$
sphere	5	3.0071E − 04	0.153 874 899	2.392 810 874
$R=1$	10	2.2449E − 12	0.156 527 151	2.383 319 427
$\kappa=4.49340945$	15	1.0175E − 14	0.156 527 163	2.383 319 428
	20	9.5447E − 15	0.156 527 163	2.383 319 428
great stellated dodecahedron	25	1.1905E − 03	−0.292 692 794	2.229 490 540
$p=4$	35	2.1864E − 04	−0.294 669 310	2.234 334 948
$\kappa=\pi$	45	5.0831E − 05	−0.294 839 844	2.232 714 273
	55	1.4777E − 05	−0.294 712 464	2.233 078 537

In this case the total exterior wave has to vanish so that the far-field pattern of the scattered wave $\boldsymbol{E}^s$ is the opposite of the far field pattern of the incident wave:

$$\boldsymbol{E}^\infty_{\text{exact}}(\widehat{\mathbf{x}})=-\frac{i\kappa}{4\pi}e^{-i\kappa\widehat{\mathbf{x}}\cdot\boldsymbol{s}}\,(\widehat{\mathbf{x}}\times\boldsymbol{p}).$$

We choosed $\boldsymbol{s}=\big(0,\frac{0.1}{\sqrt{2}},-\frac{0.1}{\sqrt{2}}\big)^\top$ and $\boldsymbol{p}=(1,0,0)^\top$. In the tabulated results we indicate the uniform-norm error (by taking the maximum of errors obtained over 1300 observed directions, i.e $n_\infty=25$) :

$$\lvert\lvert[\boldsymbol{E}^\infty_{\text{ps}}]_n-\boldsymbol{E}^\infty_{\text{exact}}\rvert\rvert_\infty=\max_{\widehat{\mathbf{x}}\in\mathbb{S}^2}\big\lvert[\boldsymbol{E}^\infty_{\text{ps}}]_n-\boldsymbol{E}^\infty_{\text{exact}}\big\rvert.$$

As a second task we compute the electric far field denoted, $\boldsymbol{E}^\infty_{\text{pw}}$, created by the scattering of an incident plane wave :

$$\boldsymbol{E}^{\text{inc}}(\mathbf{x})=\boldsymbol{p}\,e^{i\kappa\mathbf{x}\cdot\boldsymbol{d}},\quad \text{where } \boldsymbol{d},\boldsymbol{p}\in\mathbb{S}^2 \text{ and } \boldsymbol{d}\cdot\boldsymbol{p}=0.$$

In the tabulated results we indicate the real part and the imaginary part of the polarization component of the electric far field evaluated at the incident direction : $[\boldsymbol{E}^\infty_{\text{pw}}(\boldsymbol{d})]_n\cdot\boldsymbol{p}$. We choosed $\boldsymbol{d}=\big(0,0,1\big)^\top$ and $\boldsymbol{p}=(1,0,0)^\top$. In each of the examples we take $\eta=1$.

5 Numerical solution of the inverse problem and IRGNM

With the objective of using a regularized Newton-type method to solve numerically the inverse problem (1.2) we first reformulate it as a nonlinear equation posed on an open subset of admissible parametrizations of a Hilbert space. More precisely, we choose some reference domain Ω_{ref} with a simply connected closed boundary Γ_{ref} and consider mappings $\boldsymbol{q}:\Gamma_{\text{ref}}\to\Gamma$ belonging to

$$\mathcal{Q}=\{\boldsymbol{q}\in H^s(\Gamma_{\text{ref}},\mathbb{R}^3):\boldsymbol{q}\text{ injective, }\det(\mathbf{D}\boldsymbol{q}(\widehat{\mathbf{x}}))\neq 0\text{ for all }\widehat{\mathbf{x}}\in\Gamma_{\text{ref}}\}.$$

For $s > 2$ the set $\mathcal{Q}$ is open in $H^s(\Gamma_{\text{ref}}, \mathbb{R}^3)$ and $H^s(\Gamma_{\text{ref}}, \mathbb{R}^3) \subset \mathscr{C}^1(\Gamma_{\text{ref}}, \mathbb{R}^3)$. Since now, for $\boldsymbol{q} \in \mathcal{Q}$ we define $\Gamma_{\boldsymbol{q}} := \boldsymbol{q}(\Gamma_{\text{ref}})$ and denote by $\boldsymbol{n}_{\boldsymbol{q}}$ the exterior unit normal vector to $\Gamma_{\boldsymbol{q}}$. More generally we will label all quantities and operators related to the perfect conductor problem for the boundary $\Gamma_{\boldsymbol{q}}$ by the index $\boldsymbol{q}$. We denote by $F_k : \mathcal{Q} \to \boldsymbol{L}^2_{\text{t}}(\mathbb{S}^2)$ the boundary to far field operator that maps the parametrization $\boldsymbol{q}$ of the boundary $\Gamma_{\boldsymbol{q}}$ onto the far-field pattern $\boldsymbol{E}^\infty_{\boldsymbol{q},k}$ corresponding to the scattering of the incident wave $\boldsymbol{E}^{\text{inc}}_k$ by the perfect conductor $\Gamma_{\boldsymbol{q}}$. These operators may be combined into one operator $F : \mathcal{Q} \to \boldsymbol{L}^2_{\text{t}}(\mathbb{S}^2)^m, F(\boldsymbol{q}) := (F_1(\boldsymbol{q}), \ldots, F_m(\boldsymbol{q}))^\top$. We also combine the measured far-field patterns into a vector $\boldsymbol{E}^\infty_\delta := (\boldsymbol{E}^\infty_{1,\delta}, \ldots, \boldsymbol{E}^\infty_{m,\delta})^\top \in \boldsymbol{L}^2_{\text{t}}(\mathbb{S}^2)^m$ such that the inverse problem (1.2) can be written as the following nonlinear equation

$$F(\boldsymbol{q}) = \boldsymbol{E}^\infty_\delta. \tag{5.1}$$

A regularized iterative method can then be applied to the linearized equation $F'[\boldsymbol{q}]\boldsymbol{\xi} = \boldsymbol{E}^\infty_\delta - F[\boldsymbol{q}]$.

Here, we use the Iteratively Regularized Gaus-Newton Method (IRGNM). This requires to prove the Fréchet differentiability of the boundary to far-field operator F and an explicit form of the first Fréchet dérivative $F'[\boldsymbol{q}]$ and its adjoint $F'[\boldsymbol{q}]^*$. Then the iterates of the IRGNM can be computed by

$$\boldsymbol{q}^\delta_{N+1} := \text{argmin}_{\boldsymbol{q} \in H^s(\mathbb{S}^2, \mathbb{R})} \left[||F'[\boldsymbol{q}^\delta_N](\boldsymbol{q} - \boldsymbol{q}^\delta_N) + F(\boldsymbol{q}^\delta_N) - \boldsymbol{E}^\infty_\delta||^2_{\boldsymbol{L}^2} + \alpha_N ||\boldsymbol{q} - \boldsymbol{q}_0||^2_{H^s} \right], \tag{5.2}$$

Here $\boldsymbol{q}_0 = \boldsymbol{q}^\delta_0$ is some initial guess and the regularization parameters are chosen of the form $\alpha_N = \alpha_0 \left(\frac{2}{3}\right)^N$. The updates $(\partial \boldsymbol{q})_N := \boldsymbol{q}^\delta_{N+1} - \boldsymbol{q}^\delta_N$ are the unique solutions to the linear equations

$$\left(\alpha_N \mathrm{I} + F'[\boldsymbol{q}^\delta_N]^* F'[\boldsymbol{q}^\delta_N]\right)(\partial \boldsymbol{q})^\delta_N = F'[\boldsymbol{q}^\delta_N]^* \left(\boldsymbol{E}^\infty_{\kappa,\delta} - F(\boldsymbol{q}^\delta_N)\right) + \alpha_N \left(\boldsymbol{q}^\delta_0 - \boldsymbol{q}^\delta_N\right). \tag{5.3}$$

For the analysis of the derivative and its adjoint, we restrict ourselves to the case $m = 1$ since the general case can be reduced to this special case by the obvious formulas $F'[\boldsymbol{q}]\boldsymbol{\xi} = (F'_1[\boldsymbol{q}]\boldsymbol{\xi}, \ldots, F'_m[\boldsymbol{q}]\boldsymbol{\xi})^\top$ and $F'[\boldsymbol{q}]^*\boldsymbol{h} = \sum_{k=1}^m F'_k[\boldsymbol{q}]^*\boldsymbol{h}$. The following theorem is a rewriting, for the electric field only, of the theorem established in [16] by Kress.

Theorem 5.1 (characterization of $F'[\boldsymbol{q}]$). *The mapping $F : \mathcal{Q} \to \boldsymbol{L}^2_{\text{t}}(\mathbb{S}^2)$ with $s > 2$ is Fréchet differentiable at all $\boldsymbol{q} \in \mathcal{Q}$ for which $\Gamma_{\boldsymbol{q}}$ is of class $\mathscr{C}^2$, and the first derivative at $\boldsymbol{q}$ in the direction $\boldsymbol{\xi} \in H^s(\Gamma_{\text{ref}}, \mathbb{R}^3)$ is given by*

$$F'[\boldsymbol{q}]\boldsymbol{\xi} = \boldsymbol{E}^\infty_{\boldsymbol{q},\boldsymbol{\xi}},$$

where $\boldsymbol{E}^\infty_{\boldsymbol{q},\boldsymbol{\xi}}$ is the far-field pattern of the solution $\boldsymbol{E}^s_{\boldsymbol{q},\boldsymbol{\xi}}$ to the Maxwell equation (1.1a) *in $\Omega^c_{\boldsymbol{q}}$ that satisfies the Silver-Müller radiation condition and the following Dirichlet boundary condition*

$$\boldsymbol{n}_{\boldsymbol{q}} \times \boldsymbol{E}^s_{\boldsymbol{q},\boldsymbol{\xi}} = -\left(\boldsymbol{\xi} \circ \boldsymbol{q}^{-1} \cdot \boldsymbol{n}_{\boldsymbol{q}}\right) \boldsymbol{u}_{\boldsymbol{q}} \times \boldsymbol{n}_{\boldsymbol{q}} - \frac{1}{\kappa^2} \mathbf{curl}_{\Gamma_{\boldsymbol{q}}} \left((\boldsymbol{\xi} \circ \boldsymbol{q}^{-1} \cdot \boldsymbol{n}_{\boldsymbol{q}}) \operatorname{div}_{\Gamma_{\boldsymbol{q}}} \boldsymbol{u}_{\boldsymbol{q}} \right). \tag{5.4}$$

on $\Gamma_{\boldsymbol{q}}$ where $\boldsymbol{u}_{\boldsymbol{q}} = \boldsymbol{n}_{\boldsymbol{q}} \times \mathbf{curl}\left(\boldsymbol{E}^s_{\boldsymbol{q}} + \boldsymbol{E}^{\text{inc}}\right)$ and $\boldsymbol{E}^s_{\boldsymbol{q}}$ is the solution of the scattering problem (1.1a)-(1.1c) *satisfying the Dirichlet boundary condition*

$$\boldsymbol{n}_{\boldsymbol{q}} \times \left(\boldsymbol{E}^s_{\boldsymbol{q}} + \boldsymbol{E}^{\text{inc}}\right) = 0 \quad \text{on } \Gamma_{\boldsymbol{q}}.$$

To define the adjoint of $F'[\boldsymbol{q}] : H^s(\Gamma_{\text{ref}}; \mathbb{R}^3) \to \boldsymbol{L}^2_{\text{t}}(\mathbb{S}^2)$, we interpret the naturally complex Hilbert space $\boldsymbol{L}^2_{\boldsymbol{t}}(\mathbb{S}^2)$ as a real Hilbert space with the real-valued inner product $\text{Re}\langle \cdot\,, \cdot \rangle_{\boldsymbol{L}^2_{\boldsymbol{t}}(\mathbb{S}^2)}$. For bounded linear operator between complex Hilbert spaces such a reinterpretation of the spaces as real Hilbert spaces does not change the adjoint.

Proposition 5.2 (characterization of the adjoint $F'[\boldsymbol{q}]^*$). *Let*

$$\boldsymbol{E}_{\boldsymbol{h}}^{\rm inc}(\mathbf{y}) = \frac{1}{4\pi}\int_{S^2} e^{-i\kappa\widehat{\mathbf{x}}\cdot\mathbf{y}}\boldsymbol{h}(\widehat{\mathbf{x}})\,ds(\widehat{\mathbf{x}}), \qquad \mathbf{y}\in\mathbb{R}^3$$

be the vector Herglotz function with kernel $\boldsymbol{h}\in\boldsymbol{L}^2_{\rm t}(\mathbb{S}^2)$ *and* $\boldsymbol{E}_{\boldsymbol{q},\bar{\boldsymbol{h}}}$ *the total wave solution to the scattering problem for the perfectly conducting interface* $\Gamma_{\boldsymbol{q}}$ *and the incident wave* $\boldsymbol{E}_{\bar{\boldsymbol{h}}}^{\rm inc}$. *Moreover, let* $j_{\boldsymbol{H}^s\hookrightarrow\boldsymbol{L}^2}$ *denote the embedding operator from* $H^s(\Gamma_{\rm ref},\mathbb{R}^3)$ *to* $L^2(\Gamma_{\rm ref},\mathbb{R}^3)$. *Then*

$$\begin{aligned} F'[\boldsymbol{q}]^*\boldsymbol{h} \;=\; j^*_{\boldsymbol{H}^s\hookrightarrow\boldsymbol{L}^2}\Bigg(J_{\boldsymbol{q}}\Bigg(\boldsymbol{n}_{\boldsymbol{q}}\,\mathrm{Re}\Bigg\{ &-\Big(\boldsymbol{n}_{\boldsymbol{q}}\times\mathbf{curl}\,\overline{\boldsymbol{E}_{\boldsymbol{q},\bar{\boldsymbol{h}}}}\Big)\cdot\overline{\boldsymbol{u}_{\boldsymbol{q}}} \\ &+\frac{1}{\kappa^2}\,\mathrm{div}_{\Gamma_{\boldsymbol{q}}}\Big(\boldsymbol{n}_{\boldsymbol{q}}\times\mathbf{curl}\,\overline{\boldsymbol{E}_{\boldsymbol{q},\bar{\boldsymbol{h}}}}\Big)\cdot\mathrm{div}_{\Gamma_{\boldsymbol{q}}}\,\overline{\boldsymbol{u}_{\boldsymbol{q}}}\Bigg\}\Bigg)\circ\boldsymbol{q}\Bigg). \end{aligned}$$

Proof. It suffices to follow the three-step proof of Proposition 6.3 in [15]. ■

Remark 5.3 *As mentioned in [15], the implementation of the formulas in Theorem 5.1 and Proposition 5.2 is straightforward using our discretization. Indeed, by the use of the Piola transform it remains to compute some surface derivatives on* $\mathbb{S}^2$ *and both* $\mathrm{div}_{\mathbb{S}^2}$ *and* $\mathbf{curl}_{\mathbb{S}^2}$ *are diagonal with respect to the chosen bases of spherical harmonics and vector spherical harmonics.*

For the numerical experiments, we consider perfectly conducting scatterers that are star-shaped with respect to the origin. In this case, it is natural to choose the unit sphere as a reference boundary ($\Gamma_{\rm ref}=\mathbb{S}^2$) and to consider special parametrizations of the form $\boldsymbol{q}=\mathcal{R}r$ where $\big(\mathcal{R}r\big)(\widehat{\mathbf{x}})=r(\widehat{\mathbf{x}})\,\widehat{\mathbf{x}}$ for all $\widehat{\mathbf{x}}\in\mathbb{S}^2$ and r is a positive-valued function defined on the unit sphere. The function r is uniquely determined by $\Gamma_{\boldsymbol{q}}$. We restrict the set of admissible parametrization to radial parametrization and choose $\mathcal{Q}_{\rm star}=\{r\in H^s(\mathbb{S}^2,\mathbb{R}):\ r>0\}$. We have $\mathcal{R}(\mathcal{Q}_{\rm star})\subset\mathcal{Q}$, and we can define $F_{\rm star}:\mathcal{Q}_{\rm star}\to\boldsymbol{L}^2_{\boldsymbol{t}}(\mathbb{S}^2)^m$ by $F_{\rm star}:=F\circ\mathcal{R}$. Then $F_{\rm star}$ is injective if a star-shaped interface Γ is uniquely determined by the far field data $\boldsymbol{E}_1^\infty,\ldots,\boldsymbol{E}_m^\infty$. Using [12, Corollary 4] we obtain that $F'_{\rm star}[r]^*\boldsymbol{h}=j_{H^s\to L^2}r^2Re\{\ldots\}\circ\boldsymbol{q}$ where the expression in the curly brackets coincides with that in Proposition 5.2. In practice, we apply the IRGNM to the nonlinear equation $F_{\rm star}(r)=\boldsymbol{E}_\delta^\infty$. We refer to [15] for details on the inverse scattering algorithm.

Our tests concern the reconstruction of the (rounded) stellation of the dodecahedron defined by the implicit equation given in table 1. This shape consists of 20 peaks located at the 20 vertex of the regular dodecahedron. The diameter of the obstacle is roughly 2. To compute the exact far-field data we use the boundary integral equation (2.4) with $n=30$. To compute the far-field data at each iteration step we use the boundary integral equation (2.5) with $n=25$. This allows us to retrieve the boundary value data of the scattered field that are needed to evaluate the adjoint. To compute the Fréchet derivatives of the boundary to far-field operator we use the boundary integral equation (2.4). In each of the following test, we use a mesh grid of 128 ($n=7$) degrees of freedom to evaluate the far-field pattern. The radial functions describing the reconstruction belong to the space of spherical harmonics of order less than or equal to 20. The initial guess is the unit sphere. We choose $\alpha_0=10^{-2}$.

Test 1: We reconstruct the obstacle from noisy far-field measurements corresponding to the scattering of 6 incident plane waves from top, bottom, front, back, left and right. The noise level is 5%. The wavenumber κ is chosen such that the diameter of the obstacle is equivalent to the wavelength, that is $\kappa=\pi$. After ten iterations we obtain the result, presented in the top right picture below, which is pretty good. We observe that all the peaks are recovered.

Test 2: We reconstruct the obstacle from noisy far-field measurements corresponding to the scattering of one incident plane wave from bottom and polarized in the (Ox) direction. The

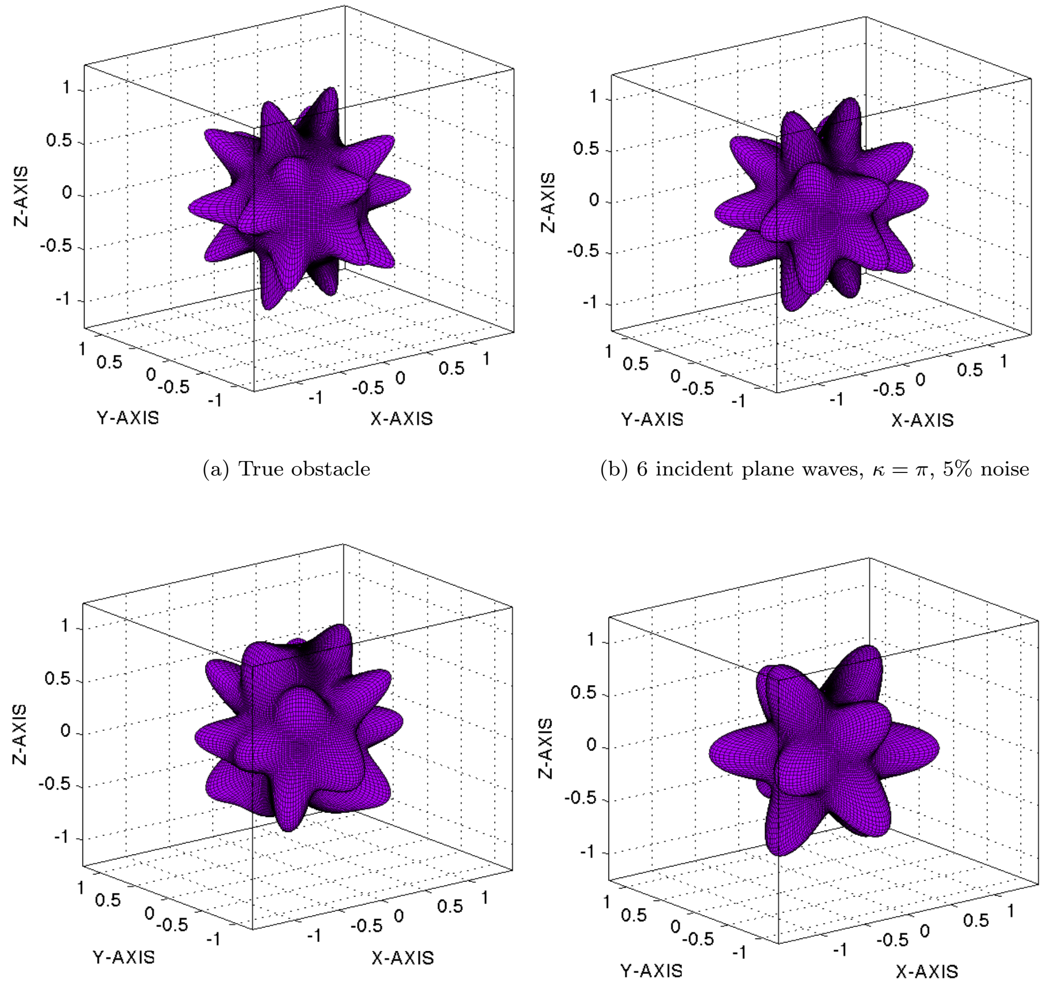

(a) True obstacle

(b) 6 incident plane waves, $\kappa = \pi$, 5% noise

(c) 1 incident plane wave, $\kappa = \pi$, 5% noise

(d) 6 incident plane waves, $\kappa = \dfrac{\pi}{2}$, 1% noise

Figure. Reconstruction of the (rounded) great stellated dodecahedron.

other parameters does not change. After twenty iterations, we obtain the result presented in the bottom left picture below.

Test 3: We reconstruct the obstacle from noisy far-field measurements corresponding to the scattering of 6 incident plane waves. The noise level is 1%. Here The wavenumber κ is chosen such that the diameter of the obstacle is greater than the wavelength, that is $\kappa = \dfrac{\pi}{2}$. After twenty iterations, we obtain the result presented in the bottom right picture below.

Acknowledgment: We would like to thank Olha Ivanyshyn and Rainer Kress for matlab code and for helpful discussions. Financial support of DFG through CRC 755 is gratefully acknowledged.

References

[1] S. Andersson, *Stellations, compounds, periodicity and the exponential scale*, preprint, Institute of Sandvik, 2004.

[2] A. B. Bakushinskiĭ, *On a convergence problem of the iterative-regularized Gauss-Newton method*, Comput. Math. Math. Phys, 32 (1992), pp. 1503–1509.

[3] D. L. Colton and R. Kress, *Integral Equation Methods in Scattering Theory*, Pure and Applied Mathematics (New York), John Wiley & Sons Inc., New York, 1983. A Wiley-Interscience Publication.

[4] ——, *Inverse acoustic and electromagnetic scattering theory*, vol. 93 of Applied Mathematical Sciences, Springer-Verlag, Berlin, second ed., 1998.

[5] M. Costabel and F. Le Louër, *On the Kleinman-Martin integral equation method for the electromagnetic scattering problem by a dielectric body*, SIAM J. Appl. Math, 27 (2011), pp. 635–656.

[6] W. Freeden, T. Gervens, and M. Schreiner, *Constructive approximation on the sphere*, Numerical Mathematics and Scientific Computation, The Clarendon Press Oxford University Press, New York, 1998. With applications to geomathematics.

[7] M. Ganesh and I. G. Graham, *A high-order algorithm for obstacle scattering in three dimensions*, J. Comput. Phys., 198 (2004), pp. 211–242.

[8] M. Ganesh and S. C. Hawkins, *A spectrally accurate algorithm for electromagnetic scattering in three dimensions*, Numer. Algorithms, 43 (2006), pp. 25–60.

[9] ——, *An efficient surface integral equation method for the time-harmonic Maxwell equations*, ANZIAM J., 48 (2007), pp. C17–C33.

[10] ——, *A hybrid high-order algorithm for radar cross section computations*, SIAM J. Sci. Comput., 29 (2007), pp. 1217–1243.

[11] ——, *A high-order tangential basis algorithm for electromagnetic scattering by curved surfaces*, J. Comput. Phys., 227 (2008), pp. 4543–4562.

[12] H. Harbrecht and T. Hohage, *Fast methods for three-dimensional inverse obstacle scattering problems*, J. Integral Equations Appl., 19 (2007), pp. 237–260.

[13] T. Hohage, *Logarithmic convergence rates of the iteratively regularized Gauss-Newton method for an inverse potential and an inverse scattering problem*, Inverse Problems, 13 (1997), pp. 1279–1299.

[14] ——, *Iterative Methods in Inverse Obstacle Scattering: Regularization Theory of Linear and Nonlinear Exponentially Ill-Posed Problems*, PhD thesis, University of Linz, 1999.

[15] T. Hohage and F. Le Louër, *A spectrally accurate method for the dielectric obstacle scattering problem and applications to the inverse problem*, in preparation, (2012).

[16] R. Kress, *Electromagnetic waves scattering : Scattering by obstacles*, Scattering, (2001), pp. 191–210. Pike, E. R. and Sabatier, P. C., eds., Academic Press, London.

[17] J.-C. Nédélec, *Acoustic and electromagnetic equations*, vol. 144 of Applied Mathematical Sciences, Springer-Verlag, New York, 2001. Integral representations for harmonic problems.

[18] S. Onaka, *Simple equations giving shapes of various convex polyhedra: The regular polydedra and polyhedra composed of crystallographically low-index planes*, Philosophical Magazine Letters, 86 (2006), pp. 175–183.

[19] M. Pieper, *Spektralrandintegralmethoden zur Maxwell-Gleichung*, PhD thesis, Georg-August-Universität Göttingen, 2007.

[20] ——, *Vector hyperinterpolation on the sphere*, J. Approx. Theory, 156 (2009), pp. 173–186.

[21] R. Potthast, *Domain derivatives in electromagnetic scattering*, Math. Methods Appl. Sci., 19 (1996), pp. 1157–1175.

[22] O. Steinbach and M. Windisch, *Modified combined field integral equations for electromagnetic scattering*, SIAM J. Numer. Anal., 47 (2009), pp. 1149–1167.